Chapter 2. Optimization of the modulation response of spatial light modulators

The key elements in the design of the real-time optical correlator that we propose are the devices used to introduce the information of the input scene and the filter. We use twisted-nematic liquid crystal spatial light modulators (TNLC SLM). The main difficulty for these devices is to uncouple the phase modulation response from the amplitude modulation response to the applied voltage, and to reach a phase modulation range of 2π. We show that this can be done by using a combination of linear polarizers and phase retarders. The incorporation of new polarization elements, such as the retarder plates, increases the degrees of freedom of the modulation system and requires a detailed analysis of the role played by each one of the elements. To do this an accurate description of polarizing devices in terms of projectors onto polarization states is proposed in this

Chapter. The introduced formalism allows us to optimize the amplitude and phase modulation response of the spatial light modulators of the correlator.

2.1. Operation curve of twisted nematic liquid crystals

In this Chapter we face the optimization of the response of the SLMs used to introduce the input scene and the filter in the real-time optical correlator. The goal is to find either configurations that provide phase only modulation regime or that provide amplitude only modulation regime.

2.1.1. *Operation curve*

The modulation response for a light modulator is characterized by its amplitude transmittance $T(V)$, that is, the ratio of the transmitted amplitude to the incident amplitude, and by its phase modulation $\tau(V)$. Both the transmittance and the phase modulation, depend on an external control parameter V, which in the case we consider, is an external voltage applied to the pixels of a TNLC panel (In other cases the control parameter is the intensity of a write-beam). One considers the complex number $\mu(V)=T(V)\exp i\tau(V)$, whose magnitude is given by the transmittance $T(V)$ and whose argument is given by the phase modulation $\tau(V)$ of the SLM, as the response of the device. As the control parameter V changes, $\mu(V)$ describes a curve in the complex plane. This curve is called the *operation curve*. We represent in Figure 2.1, three examples for typical operation curves. Figure 2.1a shows the operation curve for a coupled

amplitude and phase modulation regime, which is characterized by a spiral path on the complex plane, Figure 2.1b, and c represent the operation curve for amplitude only modulation and for phase only modulation, respectively. In the case of amplitude only modulation, the operation curve is a straight line with one extreme on the origin. The operation curve for phase only modulation is an arc of circumference centered at the origin. In the case of phase only modulation with a modulation range of 2π the operation curve is the full circumference.

Amplitude only modulation (Figure 2.1b) consists on changing the transmittance of the system, by applying an external voltage to the TNLC, keeping invariant the optical path for light that passes through it. This way one can change the magnitude of the amplitude distribution of a wave without distorting the wave front.

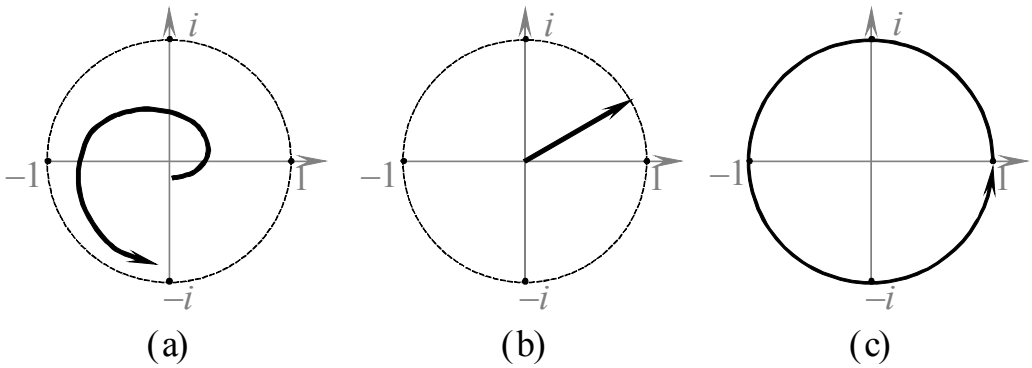

Figure 2.1. (a) Amplitude only modulation operation curve. (b) phase only modulation operation curve.

Phase only modulation is the reciprocal case. The corresponding operation curve is represented in Figure 2.1c. The optical path

of the modulation system is changed while the transmittance is kept invariant. This way one can change the wave front but the magnitude of the amplitude distribution of light is not changed.

TNLC-based SLMs present, in general, a modulation response with coupled phase and amplitude (the case in Figure 2.1a), because of the helical structure of the liquid crystal. In addition, the phase range is smaller than 2π for wavelengths in the visible range, because the new generations of TNLCs are very thin (and have low birefringence) for speed and resolution reasons.

2.1.2. *TNLC-based SLM*

We consider a spatial light modulator system that is composed by a TNLC panel placed between a linear polarizer followed by a retarder plate, and a retarder plate followed by a linear polarizer **[Márquez2001A]**, as represented in Figure 2.2.

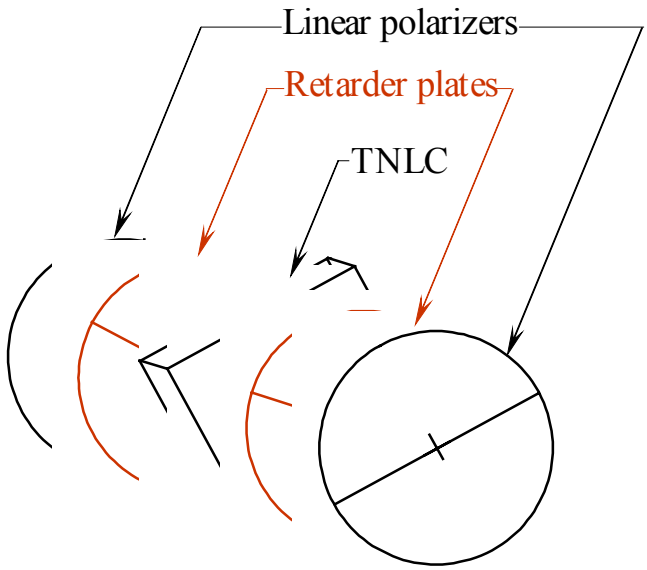

Figure 2.2. Scheme of the spatial light modulator system working with elliptically polarized light.

In such a setup, elliptic polarization states of light are generated in front of the TNLC and detected behind it. So, we call it an *elliptic light modulation setup*, in front of the usual setup without retarder plates that modulates linearly polarized light **[Moreno96] [Neto95]**.

The modulation response of the SLM to the voltage applied to the TNLC, is determined by the six parameters that configure the polarizing elements. They are, the orientation of the transmission axes of the two linear polarizers, the orientation of the axes of the two retarder plates, and the retardance for the two retarder plates, that can be different.

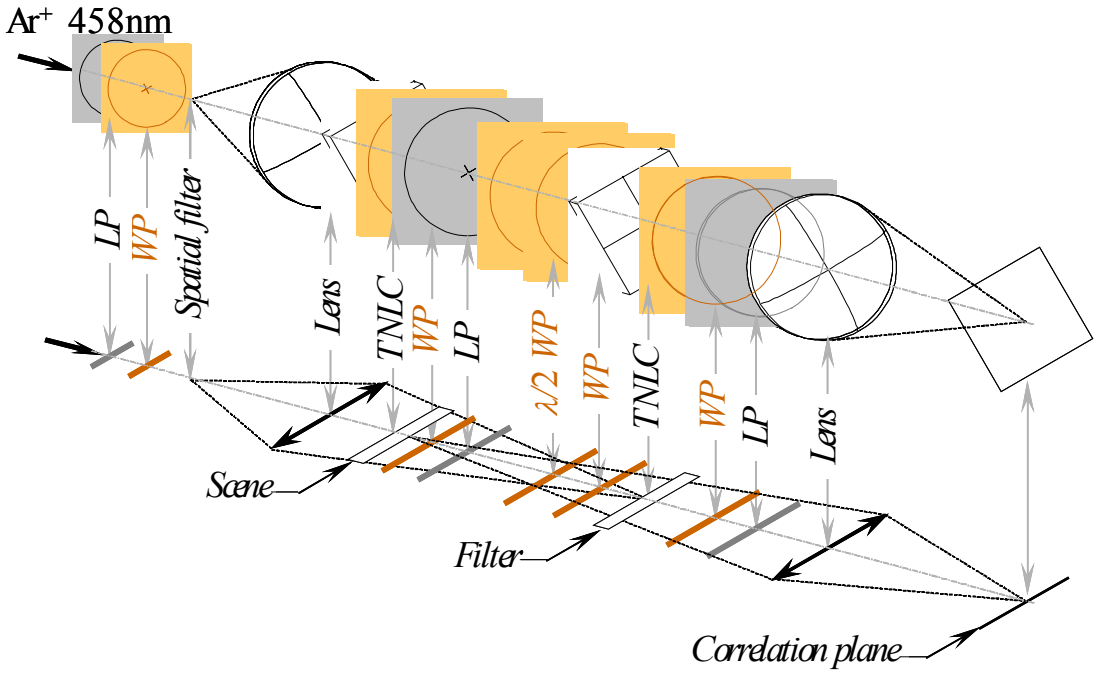

Figure 2.3. Polarization elements of the optical correlator.

In the optical correlator we propose, we use TNLC-based spatial light modulators to implement both the scene and filter. In both cases we consider elliptic light modulation setups. We show in Figure 2.3 the scheme of the optical correlator, with the polarization devices involved in the spatial light modulators (SLMs) for the scene and the filter. The linear polarizer and the retarder plate corresponding to the input of the scene TNLC are placed before the spatial filter, this way, small aperture plates can be used. After the scene, there are the retarder plate and linear polarizer corresponding to the output of the scene. Because after the mentioned polarizer, the light is linearly polarizer, we have replaced the polarizer corresponding to the input of the filter TNLC by a half wave plate. This plate simply rotates the vibration plane of the light, without absorbing any component. This way, the required linear polarization state at the desired orientation can be obtained. Finally, a retarder plate and a linear polarizer are placed after the filter TNLC.

In the correlator we propose, the scene SLM works either in amplitude only modulation regime, or in phase only modulation regime. The filter SLM works in phase only regime. Therefore, it is necessary to find the configuration of the polarizing elements of the SLMs (orientation angles and retardances) that provide the corresponding modulation responses, or at least the most approximate responses. This is done by an optimization process.

The optimization of the modulation is performed by maximizing a merit function defined to evaluate the proximity of a given operation curve to the desired modulation. The trajectory of the operation curve on the complex plane is determined by the configuration parameters of the polarizers and phase retarders of the optical system. This way, to optimize the modulation response consists on maximizing the merit function as a function of the configuration parameters **[Márquez2001A].** Such a function depends on the physical model of the elements involved in the setup, including the TNLC panel. Therefore, it is critical to have an accurate model of the TNLC panel that characterizes its polarization behavior, and capable to predict the trajectory on the complex plane of the operation curve as a function of the configuration angles and retardances of the system.

We propose to take into account some new additional considerations for the optimization. Let us analyze the modulation of the SLM system in detail.

The first linear polarizer and retarder plate generate an elliptic polarization state. This polarization state is then transformed by the TNLC onto another polarization state which depends on the voltage. Finally, one elliptical component of this voltage-dependent polarization state is selected by the retarder plate and linear polarizer behind the TNLC. That means that, once the TNLC is selected, the modulation is determined by the polarization state generated at the input of the TNLC and the

polarization state selected at the output. That is, the modulation is determined by two polarization states, and because each polarization state is determined by two parameters (such as the orientation and ellipticity of the polarization ellipse), the modulation is determined by four free parameters. Consequently, the merit function for the optimization can be expressed as a function of four free parameters, instead of six parameters.

Therefore, we propose to approach the analysis of the modulation from the point of view of the polarization states in front of and behind the TNLC, instead of the operators of the devices used to generate and detect them. And then to find the configuration of the polarizers and retarders that generate these polarization states.

To determine how the amplitude and phase modulation depend on the polarization states it is necessary to determine how the wave information is contained in polarization states. We will introduce a notation of Jones' vectors **[Jones41]** in which the wave information and the polarization information are separated in two factors, that express separately the wave information and the polarization information. This notation will be used to demonstrate that the amplitude and phase modulation of the SLM depends on the polarizer and retarder parameters only through the polarization state they generate and/or detect.

We will also use Poincaré's sphere **[Jerrard54] [Huard94]** to determine and interpret the relations between the polarization states and the polarization devices used to generate and detect them. We will show which conditions must be satisfied by the retarder plates and the polarizers to be able to generate a given polarization state.

Once the modulation is expressed in terms of polarization states, the optimization process can be performed in terms of the four free parameters that determine these states, for example the orientation and ellipticity for the generated and detected polarization states.

The procedure will be used to obtain an amplitude only configuration for the scene SLM of the correlator. We will define the merit function for this modulation regime and we will describe the optimization algorithm. We will use a procedure based on the same optimization algorithm but using a different merit function to obtain the optimal phase only modulation configuration for both the scene SLM and the filter SLM.

2.2.Wave properties of polarized states of light.

Jones vectors are revealed to be a powerful tool for describing polarization states and devices. Polarization states are described by complex-component vectors of dimension two, while devices are described by complex component matrices. This way the

polarization characteristics of a composed system is easily obtained by the matrix product of the parts.

In this section we are going to show how not only the polarization state is described by the Jones vector but also the wave information.

2.2.1. *Vector description of polarization states.*

Let us consider a monochromatic electromagnetic plane wave, propagating in the vacuum along the direction of the *z*-axis. The electric displacement field is described by the following vector **D**(*z*,*t*):

$$\mathbf{D}(z,t) = A_x \exp[i(kz - \omega t + \phi_x)]\mathbf{u}_x + A_x \exp[i(kz - \omega t + \phi_y)]\mathbf{u}_y \qquad (2.1)$$

One can write this expression as the product of two factors as follows.

$$\mathbf{D}(z,t) = \left(A_x \exp i\phi_x \mathbf{u}_x + A_y \exp i\phi_y \mathbf{u}_y\right)\exp[i(kz - \omega t)] \qquad (2.2)$$

One of the factors (exp[i(kz−ωt)]) determines the space-time dependency of the field. The other factor is a complex-component vector that characterizes the direction and amplitude of the oscillations of the electric displacement field in the plane orthogonal to the propagation direction, or in other words, the *polarization* of the light. One calls this vector a *Jones vector* **[Jones41]**, which is usually represented by a column-vector as follows:

$$|A\rangle = \begin{bmatrix} A_x \exp i\phi_x \\ A_y \exp i\phi_y \end{bmatrix}. \qquad (2.3)$$

We use Dirac ket vectors $|\ \rangle$ to designate Jones vectors.

2.2.2. *Wave information and polarization information*

The amplitude and phase of the components of the Jones vector determine the amplitude and phase delay with respect to an arbitrary origin of the electric displacement field. This is represented in Figure 2.4. Let us remark that aside from the space-time dependency, determined by **k** and ω, monochromatic plane waves are completely determined by the components of their corresponding Jones vector. In particular, the intensity of the polarization state described by a Jones vector is given by the hermitian scalar product of the Jones vector, as follows:

$$A^2 = \langle A|\, A\rangle = A_x^{\,2} + A_y^{\,2}. \qquad (2.4)$$

In a fixed point of the space, the electric displacement **D** describes an ellipse on the x,y plane, which is the particular case of Lissajous curve for two harmonic components with the same frequency. While the Jones vector has four degrees of freedom, the polarization ellipse is completely determined by only two parameters, i.e. the ratio between the two components of the electric field (see angle χ in Figure 2.4) and their phase difference (represented as ϕ in Figure 2.4). Then, it results

convenient to write the Jones vector as the product of a complex coefficient, that carries the amplitude and absolute phase of the electromagnetic wave, and a unit vector, that depends uniquely on the angles χ and ϕ, and that describes completely the polarization state, as follows:

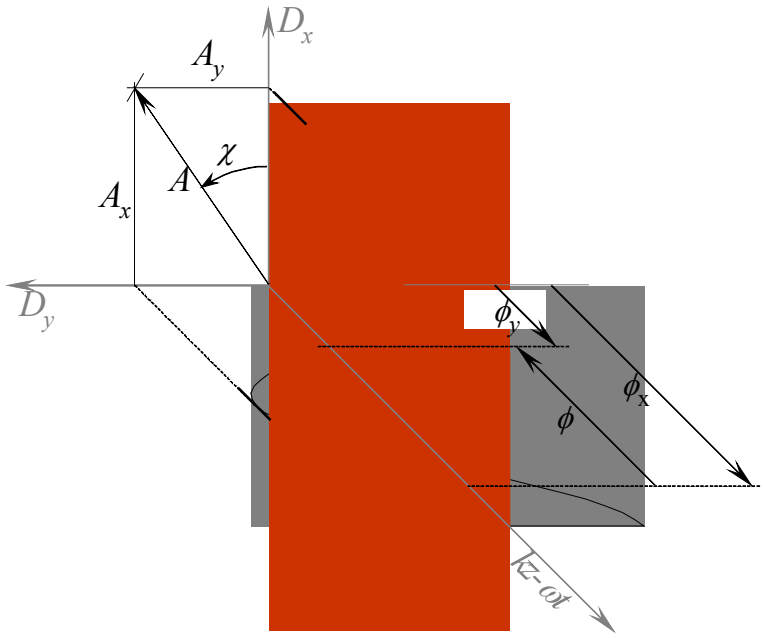

Figure 2.4. Representation of the magnitude and phase of the components of a Jones vector as parameters of the harmonic components of the propagating electric displacement field.

$$|A\rangle = A\exp i\phi_x |\chi,\phi\rangle, \tag{2.5}$$

$|\chi,\phi\rangle$ is a unit vector with components

$$|\chi,\phi\rangle = \begin{bmatrix} \cos\chi \\ \exp i\phi \sin\chi \end{bmatrix}, \tag{2.6}$$

where

$$\chi = \arctan\frac{A_y}{A_x}, \text{ and } \phi = \phi_y - \phi_x \qquad (2.7)$$

are parameters that completely determine the polarization ellipse, and therefore determine how the polarization state is affected by linear polarizing devices, like polarizers, retarder plates or TNLCs. In Table 2.1 we give the values of χ and ϕ, the corresponding Jones matrices and the polarization ellipse, for the main polarization states. According to Figure 2.4 the linear polarization along the vertical of the laboratory (x axis in Figure 2.4) is represented by the state $|0,0\rangle$.

$\lvert\chi,\phi\rangle$	Matrix	Ellipse	$\lvert\chi,\phi\rangle$	Matrix	Ellipse
$\lvert 0,0\rangle$	$\begin{bmatrix}1\\0\end{bmatrix}$		$\lvert \frac{\pi}{2},0\rangle$	$\begin{bmatrix}0\\1\end{bmatrix}$	
$\lvert \frac{\pi}{4},0\rangle$	$\frac{1}{\sqrt{2}}\begin{bmatrix}1\\1\end{bmatrix}$		$\lvert \frac{3\pi}{4},0\rangle$	$\frac{1}{\sqrt{2}}\begin{bmatrix}1\\-1\end{bmatrix}$	
$\lvert \frac{\pi}{4},\frac{\pi}{2}\rangle$	$\frac{1}{\sqrt{2}}\begin{bmatrix}1\\i\end{bmatrix}$		$\lvert \frac{3\pi}{4},\frac{\pi}{2}\rangle$	$\frac{1}{\sqrt{2}}\begin{bmatrix}1\\-i\end{bmatrix}$	

Table 2.1. Values of χ, ϕ, Jones matrices and polarization ellipse for the main polarization states

The magnitude A and phase ϕ_x of the complex coefficient determine the scale of the ellipse and the position of the electric field on the ellipse when $kz-\omega t=0$, respectively. These parameters must be considered for wave superposition problems, like interference or diffraction. Let us say, they carry the wave information of the propagating field.

Then, Jones vector describes both, wave properties, like the amplitude and phase at a given point, and the polarization characteristics, which determine the effect of the different polarizing elements on the polarization of light.

A useful analogy to understand the way in which the wave information and polarization information are contained in a Jones vector is by thinking on the Jones vector space as a regular geometrical space. In a real-component vector space any vector can be written as a scalar number multiplied by a unit vector. The scalar number represents the length of the vector, and the unit vector gives the direction of the vector in the space. Jones vectors have complex components, and therefore they do not have a direct geometrical interpretation, but in any case we can write them as the product of a scalar, that carries the wave information, by a unit vector, that carries the polarization information. Therefore we would say that the polarization state information carried by a Jones vector is determined by its "direction" in the Jones vector space and the wave properties are determined by its "length", which is complex valued.

2.3.Jones vectors and polarization states

The *Jones vector space*, noted $\mathbb{J}$, is the ensemble of all possible Jones vectors, which represent all the possible polarization

states of monochromatic light with all the possible wave states[†]. It is a two dimensional vector space over the complex field. Because it is two dimensional, any couple of linearly independent vectors constitutes a basis of the vector space. However, we will consider only orthonormal bases, that is, bases of unit vectors which are orthogonal each other.

2.3.1. *Components of a polarization state on a base*

Let us consider two orthonormal polarization states, $|e_+\rangle$ and $|e_-\rangle$, because $|e_+\rangle$ and $|e_-\rangle$ are linearly independent each other and the dimension of $\mathbb{J}$ is two, any vector $|A\rangle$ can be written as a linear combination of them.

$$|A\rangle = A_+|e_+\rangle + A_-|e_-\rangle . \tag{2.8}$$

And because $\{|e_+\rangle,|e_-\rangle\}$ is an orthonormal basis we have $A_+=\langle e_+|A\rangle$ and $A_-=\langle e_-|A\rangle$. Therefore we can write the identity operator as follows:

$$\mathbf{I} = |e_+\rangle\langle e_+| + |e_-\rangle\langle e_-| . \tag{2.9}$$

Here $\langle e_+|$, $\langle e_-|$represent the elements of the basis of the dual space of $\mathbb{J}$, noted as $\mathbb{J}^*$, which is the vector space composed by linear applications between $\mathbb{J}$ and the field of complex numbers.

[†] Aside from the space-time dependency of the wave, determined by **k** and ω.

We say that $\langle e_+|$ is the dual form of $|e_+\rangle$, because it represents the linear operator that applied to any vector $|A\rangle$ gives the scalar product $\langle e_+|A\rangle$.

2.3.2. *Poincaré's sphere representation of polarization states.*

Poincaré's sphere is a representation of polarization states (considering unit intensity states) in which the (geodesic) distance between points constitutes a measure of the similarity between the polarization states represented by them. Any polarization state $|\chi,\phi\rangle$ (see equation 2.6) is represented by one unique point on Poincaré's sphere. whose Cartesian coordinates, s_1, s_2, and s_3 are given by

$$s_1(\chi,\phi) = \cos 2\chi . \tag{2.10a}$$

$$s_2(\chi,\phi) = \sin 2\chi \cos\phi . \tag{2.10b}$$

$$s_3(\chi,\phi) = \sin 2\chi \sin\phi . \tag{2.10c}$$

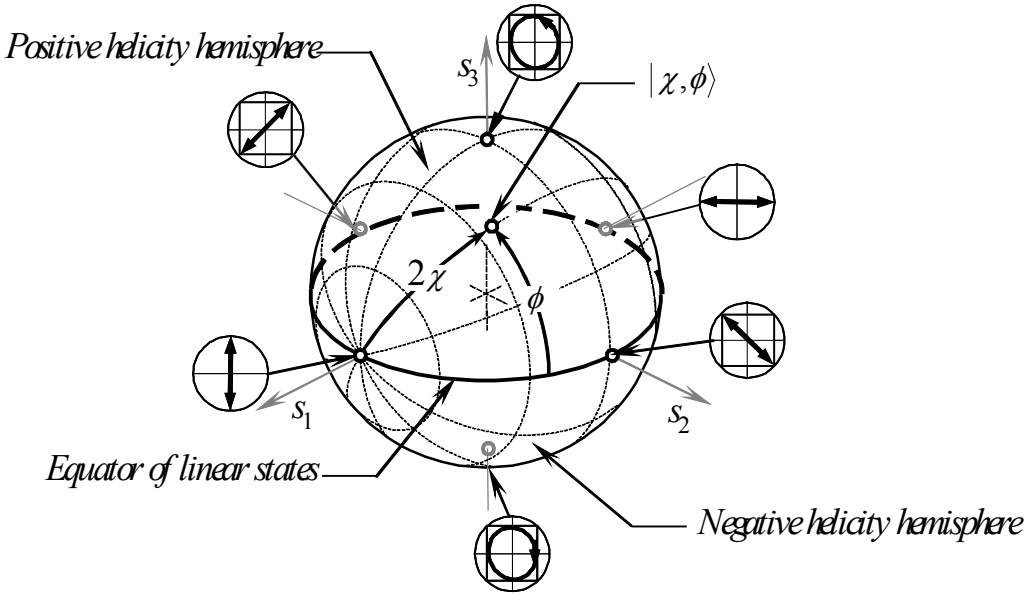

Figure 2.5. Representation of the principal polarization state on Poincaré's sphere.

This way, 2χ and ϕ can be considered as the polar and azimuth angle of a coordinate system on the sphere in which the poles are the horizontal and vertical linear polarization states, that are represented by the intersection of the sphere with the s_1 axis (see Figure 2.5). The polarization states are distributed on Poincaré's sphere as represented in Figure 2.5. The sphere is divided in two hemispheres by the maximum circle corresponding to ϕ=0 (or π). This circle, which is the intersection of the sphere with the s_1s_2 plane is represented in Figure 2.5 by a solid black line. It corresponds to the linear polarization states for all the directions, and states polarized along orthogonal directions are represented by antipode points. Vertical and horizontal polarization states are on the s_1-axis, and polarization at 45 and -45 degrees are on the s_2-axis.

All the points on the hemisphere with positive value of s_3 represent states with positive helicity. These are the left-handed elliptic polarization states and the left circular polarization state, which is represented on the s_3-axis. The hemisphere for negative values of s_3 correspond to the states with negative helicity, that is the right-handed elliptic states, and the right circular polarization.

2.3.3. *Ellipticity and orientation parameterization of polarization states.*

From the geometrical point of view, it seems natural to establish a parameterization in which the poles are the two circular states (axis s_3), and the equator represents all the linear states, and divides the sphere in two hemispheres, one for the left-handed states and the other for the right-handed ones.

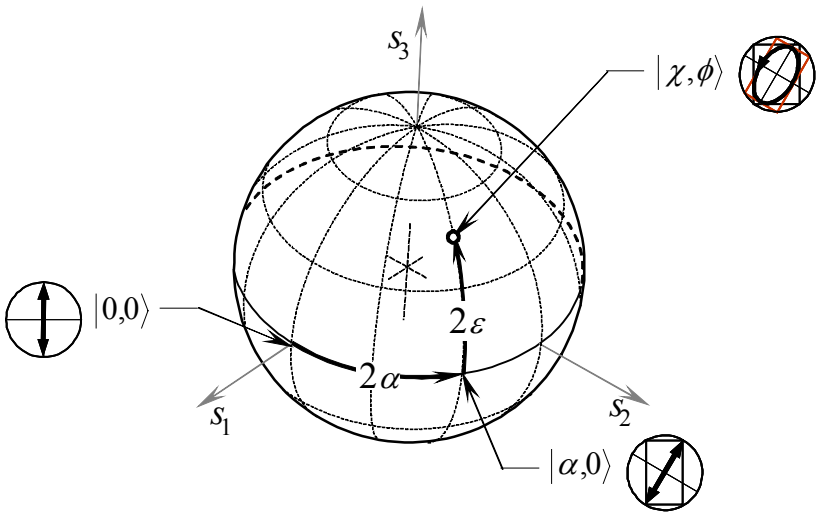

Figure 2.6. Parameterization of Poincaré's sphere in terms of ellipticity and orientation.

Therefore we can define a couple of parameters 2α and 2ε as follows:

$$\begin{aligned} 2\varepsilon &= \arcsin s_3 \\ 2\alpha &= \arctan\frac{s_2}{s_1} \end{aligned} \quad . \tag{2.11}$$

This way, Poincaré's sphere is parameterized as shown in Figure 2.6. That is the two poles represent the circular states, and the equator of linear states, divides the sphere in the hemispheres of the right-handed and the left-handed states.

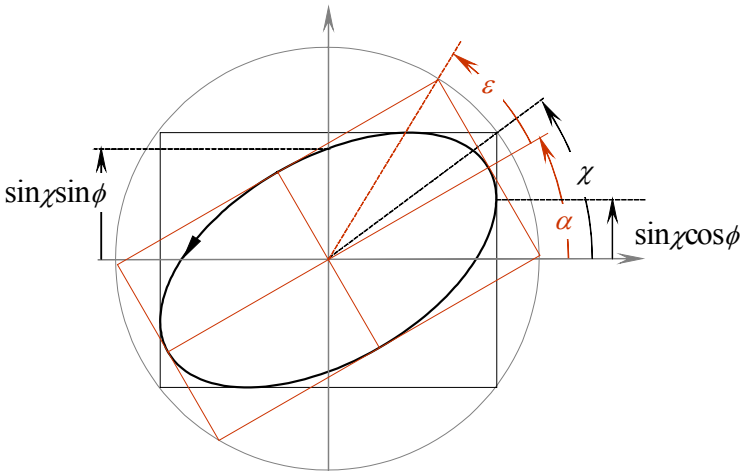

Figure 2.7. Geometrical parameters of the polarization ellipse. Black lines correspond to the χ, ϕ parameters and red lines correspond to the α and ε parameters.

Here 2ε takes values between $-\pi/2$ and $+\pi/2$ and its sign corresponds to the helicity of the polarization state. We represent in Figure 2.7 the polarization ellipse for the polarization state $|\chi,\phi\rangle$ together with the geometrical parameters α and ε. α gives the orientation of the major axis of the polarization ellipse, therefore it is called the *orientation angle*. ε is the angle whose tangent gives the ratio of the minor axis to

the major axis. It determines the ellipticity of the polarization state, therefore it is known as the *ellipticity angle*.

2.3.4. *Relation between α,ε and χ,ϕ*

The relation between the different parameterizations of Poincaré's sphere is given by the following equation:

$$|\chi,\phi\rangle = \mathbf{R}(\alpha)\left|\varepsilon,\tfrac{\pi}{2}\right\rangle, \qquad (2.12)$$

where $\mathbf{R}(\alpha)$ is the rotation matrix. We represent in Figure 2.8 the $\chi,\phi,\alpha,\varepsilon$ parameters for a given polarization state on Poincaré's sphere. The state $|\chi,\phi\rangle$, together with the states $|0,0\rangle$ and $|\alpha,0\rangle$ form a spherical triangle with sides 2χ, 2α and 2ε. The angle opposite to 2χ is a right angle and the angle opposite to 2ε is ϕ. This triangle can be solved by spherical trigonometry rules.

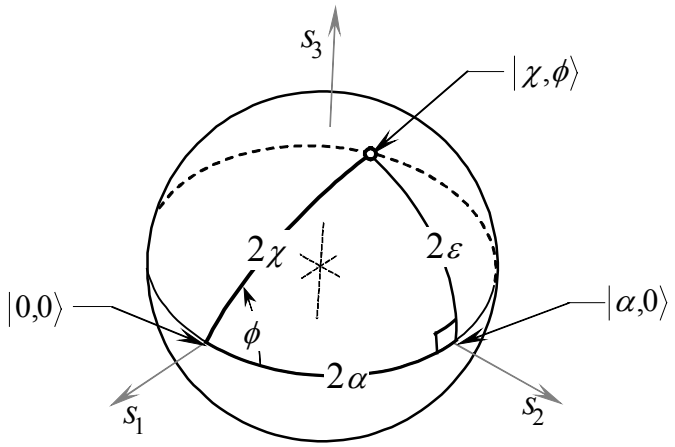

Figure 2.8. Spherical triangle formed by the different parameterizations of a given state in Poincaré's sphere.

By applying the cosine rule we have the following relation

$$\cos 2\chi = \cos 2\alpha \cos 2\varepsilon\,. \qquad (2.13)$$

And by the sine rule we have

$$\sin\phi = \frac{\sin 2\varepsilon}{\sin 2\chi}. \tag{2.14}$$

And from these relations we can obtain the expression of χ and ϕ as functions of α and ε:

$$\begin{aligned} \cos 2\chi &= \cos 2\alpha \cos 2\varepsilon \\ \tan\phi &= \sin 2\alpha \tan 2\varepsilon \end{aligned}, \tag{2.15}$$

and also the inverse relations:

$$\begin{aligned} \sin 2\varepsilon &= \sin 2\chi \sin\phi \\ \tan 2\alpha &= \cos\phi \tan 2\chi \end{aligned}. \tag{2.16}$$

Both representations are useful: (2χ,ϕ) give immediate information on the amplitude ratio, and phase difference between the two components of a polarization state in a given frame, while (2α,2ε) directly determine the geometrical properties of the polarization ellipse.

2.3.5. *Representation of unitary transformations on Poincaré's sphere*

Transformations between polarization states have their corresponding representation on Poincaré's sphere. In particular we consider unitary transformations, and because any unitary transformation can be decomposed in terms of rotations and phase shifts **[Jones41]** we consider only these kind of transformations.

Let us consider a rotation $\mathbf{R}(\theta)$ applied to a polarization state whose orientation and ellipticity angles are α and ε, respectively. Whatever the ellipticity of the state is, the resulting state has the same ellipticity, and increments its orientation by an angle θ. Therefore, the resulting state can be represented on Poincaré's sphere by applying a rotation of 2θ about the s_3 axis to the point that represents the input state. We represent in Figure 2.9a some of the trajectories, parameterized by 2θ, defined by the points that represent the polarization states resulting from the rotation by an angle θ. These trajectories are always parallel to the equator of linear states. As expected, circular polarization states are unaltered for any rotation angle.

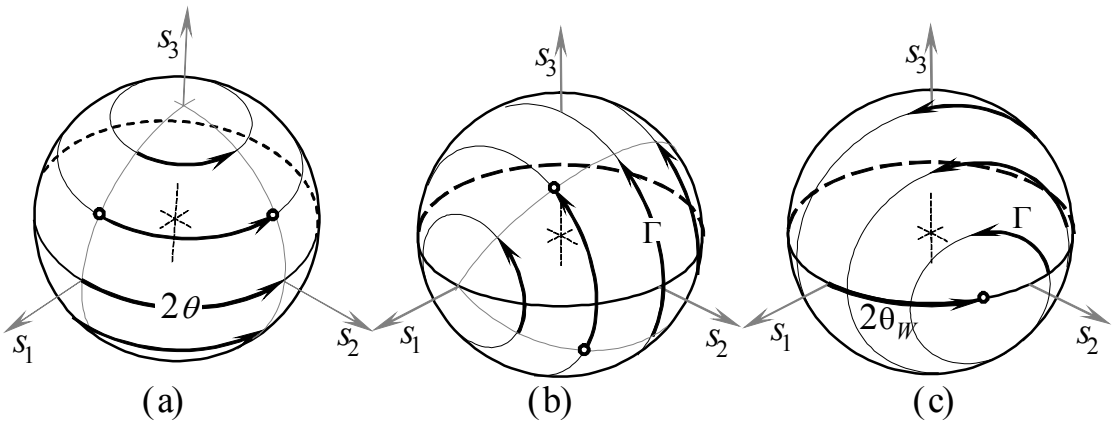

Figure 2.9. Representation on Poincaré's sphere of the transformation of polarization states induced by (a) rotations, (b) phase retarders with the neutral axes on the x,y axes, and (c) at an arbitrary orientation.

Let us now consider the representation for a retarder plate with the neutral axes along the x and y axes, and with retardance Γ. A given polarization state $|\chi,\phi\rangle$, that is, a state whose components have a phase delay ϕ, is transformed onto the polarization state $|\chi,\phi+\Gamma\rangle$. Note that the retarder plate does not change the ratio

between the components of the polarization state. This is represented on Poincaré's sphere by a rotation about the s_1 axis by an angle Γ, which is the axis that contains the liner polarization states along x and y.(see Figure 2.9b). Note that the linear states along the x and y axes of the laboratory are not changed by the phase retarder.

Any other orientation of a retarder plate can be understood as the composition of a retarder plate with the neutral axes along the coordinate axes and two rotations as follows $\mathbf{W}(\Gamma,\theta_W)=\mathbf{R}(-\theta_W)\mathbf{W}(\Gamma,0)\mathbf{R}(\theta_W)$. That means that the representation in Poincaré's sphere of the transformation corresponding to a retarder plate with an arbitrary orientation θ_W, is obtained from the composition of two rotations about the s_3 axis and one rotation about the s_1 axis. Therefore $\mathbf{W}(\Gamma,\theta_W)$ is also represented by a rotation. In addition, let us note that the retarder plate does not alter the linear states $|\theta_W,0\rangle$ and $|\theta_{W\perp},0\rangle$. Then, these states determine the rotation axis of the representation in Poincaré's sphere of the retarder plate, as represented in Figure 2.9c.

2.4.polarization state generator and detector.

2.4.1. *Linear polarizer and phase retarder in Dirac notation*

The operators for linear polarizers and for phase retarders can also be written using Dirac notation. This way, an expression that is independent of the chosen frame is obtained.

Let us consider the operator for a linear polarizer with its transmission axis at an angle θ_P to the x axis of the laboratory frame. The operator is given by next expression:

$$\mathbf{P}(\theta_P) = \mathbf{R}(\theta_P)\mathbf{P}(0)\mathbf{R}(-\theta_P). \tag{2.17}$$

Here **P**(0) is the operator that fully transmits the linear polarization along the x-axis, denoted as $|0,0\rangle$ and fully extinguishes the polarization along the y-axis, given by $|\pi/2,0\rangle$. We compose **P**(0) operator with the identity operator **I**, expressed as equation 2.9 indicates, then we have:

$$\begin{aligned}\mathbf{P}(\theta_P) = {} & \mathbf{R}(\theta_P)\mathbf{P}(0)|0,0\rangle\langle 0,0|\mathbf{R}(-\theta_P) \\ & + \mathbf{R}(\theta_P)\mathbf{P}(0)\left|\tfrac{\pi}{2},0\right\rangle\left\langle\tfrac{\pi}{2},0\right|\mathbf{R}(-\theta_P)\end{aligned}. \tag{2.18}$$

The second term is null because $\mathrm{P}(0)|\pi/2,0\rangle$ is zero. Then we have:

$$\begin{aligned}\mathbf{P}(\theta_P) = {} & \mathbf{R}(\theta_P)|0,0\rangle\langle 0,0|\mathbf{R}(-\theta_P) \\ = {} & |\theta_P,0\rangle\langle\theta_P,0|\end{aligned}. \tag{2.19}$$

That is, the polarizer can be represented by a orthogonal projector operator that selects the orthogonal projection of the input state onto the state $|\theta,0\rangle$. Let us note that the usual Jones matrix for the linear polarizer can be obtained by performing the explicit product $|\theta_P,0\rangle\langle\theta_P,0|$, as follows:

$$|\theta_P,0\rangle\langle\theta_P,0| = \begin{bmatrix}\cos\theta_P \\ \sin\theta_P\end{bmatrix}\begin{bmatrix}\cos\theta_P & \sin\theta_P\end{bmatrix} = \begin{bmatrix}\cos^2\theta_P & \cos\theta_P\sin\theta_P \\ \cos\theta_P\sin\theta_P & \sin^2\theta_P\end{bmatrix}. \tag{2.20}$$

A similar argument can be used for the retarder plate operator. In this case we obtain the following relation,

$$\mathbf{W}(\Gamma,\theta_W) = |\theta_W,0\rangle\langle\theta_W,0| + \exp i\Gamma\,|\theta_{W\perp},0\rangle\langle\theta_{W\perp},0|. \tag{2.21}$$

Here, Γ is the retardance of the retarder plate, θ_W is the angle of its slow axis to the x frame of the laboratory axis, and $\theta_{W\perp}=\theta_W+\pi/2$. This way, when the operator is applied to an arbitrary state $|A\rangle$ the component onto the linear state $|\theta_{W\perp},0\rangle$ is forwarded by a phase Γ respect to the component onto the linear state $|\theta_W,0\rangle$.

2.4.2. *On-axis polarization state generator*

Let us consider a system composed of a linear polarizer at an angle $\theta_P=\chi$ to the x-axis of the laboratory frame followed by a phase retarder with retardance $\Gamma=\phi$, with the slow axis along the x-axis of the laboratory frame ($\theta_W=0$). The operator that characterizes the system is described by the operator

composition $\mathbf{W}(\phi,0)\mathbf{P}(\chi)$. This operator can however be written as follows:

$$\mathbf{W}(\phi,0)\mathbf{P}(\chi)=\left[|0,0\rangle\langle 0,0|+\exp i\phi\,|\tfrac{\pi}{2},0\rangle\langle\tfrac{\pi}{2},0|\right]|\chi,0\rangle\langle\chi,0|\,. \qquad (2.22)$$

If this operator is developed, it can be written as

$$\mathbf{W}(\phi,0)\mathbf{P}(\chi)=\left[|0,0\rangle\langle 0,0|\chi,0\rangle+\exp i\phi\,|\tfrac{\pi}{2},0\rangle\langle\tfrac{\pi}{2},0|\chi,0\rangle\right]\langle\chi,0|\,. \qquad (2.23)$$

And by realizing that $\langle 0,0|\chi,0\rangle=\cos\chi$ and $\langle\pi/2,0|\chi,0\rangle=\sin\chi$ we have

$$\mathbf{W}(\phi,0)\mathbf{P}(\chi)=\left[\cos\chi|0,0\rangle+\exp i\phi\sin\chi|\tfrac{\pi}{2},0\rangle\right]\langle\chi,0|\,. \qquad (2.24)$$

That can be compactly written as follows

$$\mathbf{W}(\phi,0)\mathbf{P}(\chi)=|\chi,\phi\rangle\langle\chi,0|\,. \qquad (2.25)$$

That is, this combination of linear polarizer and retarder plate transforms the linear polarization state $|\chi,0\rangle$ onto $|\chi,\phi\rangle$. Whatever the illumination is, the system generates a polarization state proportional to $|\chi,\phi\rangle$. So, we call this system a *Polarization State Generator* (PSG).

An scheme of PSG is presented in Figure 2.10. When the light passes through the linear polarizer, a polarization state described by a Jones vector proportional to the linear state $|\chi,0\rangle$ is obtained. Because the state is a linear state, both linear components $\langle 0,0|\chi,0\rangle$ and $\langle\pi/2,0|\chi,0\rangle$ have the same phase. However, when the light passes through the retarder plate the

phase of the two components is changed by different amounts, and therefore, an elliptic polarization state $|\chi,\phi\rangle$ is obtained.

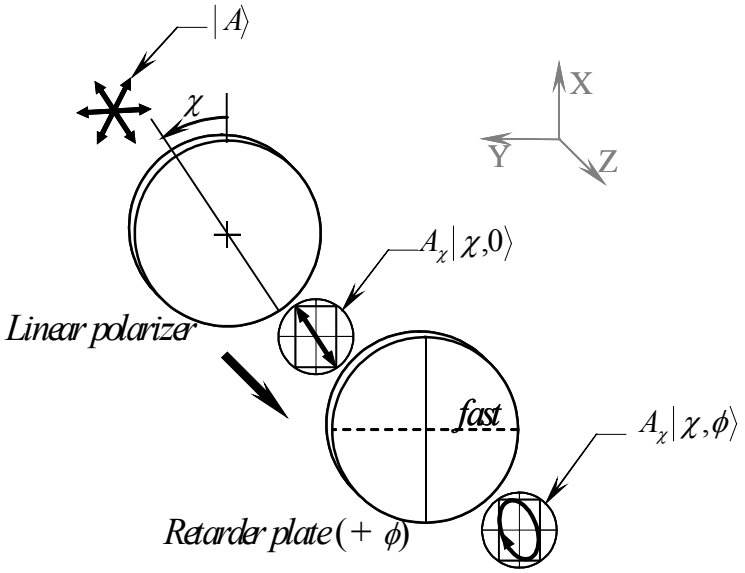

Figure 2.10. Illustration of a polarization state generator composed by a linear polarizer and a phase retarder plate.

Note that the polarization state orthogonal to $|\chi,\phi\rangle$ can be generated by simply rotating the linear polarizer by 90 degrees to the angle χ.

2.4.3. *On axis polarization state detector*

Similarly to the case of the PSG system, we can write the operator of a system composed by a retarder plate followed by a linear polarizer in terms of a tensorial product of polarization states.

$$\mathbf{P}(\chi)\mathbf{W}(-\phi)=|\chi,0\rangle\langle\chi,\phi|\,. \tag{2.26}$$

That is, this system detects the projection of the input polarization state onto the state $|\chi,\phi\rangle$ and transforms it onto the

linear state $|\chi,0\rangle$, with an amplitude and phase that correspond to those of the projection of the input state onto $|\chi,\phi\rangle$. In addition, the state $|\chi_\perp,\phi\rangle$ is totally extinguished, therefore this system is called a *polarization state detector* (PSD). We represent a scheme of polarization state detector in Figure 2.11. We consider an arbitrary polarization state as a linear combination of $|\chi,\phi\rangle$ and its orthogonal $|\chi_\perp,\phi\rangle$. When these states pass through the retarder plate, the phase difference between the two linear components of the basis states is compensated and they are transformed onto two orthogonal linear states at angles χ and $\chi_\perp$ respectively. Because the linear polarizer has its transmission axis at χ, only one of these states (multiplied by its corresponding component) is transmitted. Let us remark that the amplitude and the phase of the output linear state are given by the magnitude and argument of the component of the input state onto the state $|\chi,\phi\rangle$.

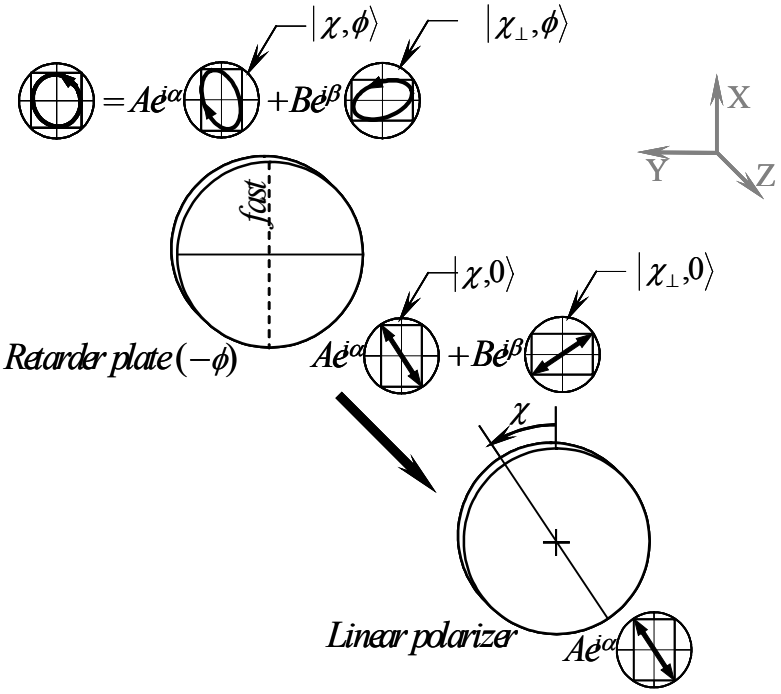

Figure 2.11. Illustration of a polarization state detector composed by a phase retarder plate followed by a linear polarizer.

2.4.4. *Off-axis polarization state generator and detector*

As far, we have just considered PSG and PSD systems in which the retarder plate has the neutral axes aligned to the x and y axes of the reference frame. Any other case can be considered as a rotation of these systems. This is expressed as follows:

$$\begin{aligned}&\mathbf{W}(\Gamma,\theta_W)\mathbf{P}(\theta_P)=\mathbf{R}(\theta_W)\mathbf{W}(\Gamma)\mathbf{P}(\theta_P-\theta_W)\mathbf{R}(-\theta_W)\\&=\mathbf{R}(\theta_W)\left|\theta_P-\theta_W,\Gamma\right\rangle\left\langle\theta_P-\theta_W,0\right|\mathbf{R}(-\theta_W)\end{aligned}. \qquad (2.27)$$

Here θ_P and θ_W are the orientation of the linear polarizer and the retarder plate, respectively, and Γ is the retardance of the wave plate. These three parameters characterize the PSG.

Because the generated polarization state is still determined by two parameters one can write

$$\mathbf{W}(\Gamma,\theta_W)\mathbf{P}(\theta_P) = |\chi,\phi\rangle\langle\theta_P|, \tag{2.28}$$

and the relation between the PSG parameters and the state parameters is given by

$$|\chi,\phi\rangle = \mathbf{R}(\theta_W)|\theta_P - \theta_W,\Gamma\rangle. \tag{2.29}$$

To solve this equation, which is a system of coupled trigonometric functions we use the representation of polarization states and operators in Poincaré's sphere (see Figure 2.12).

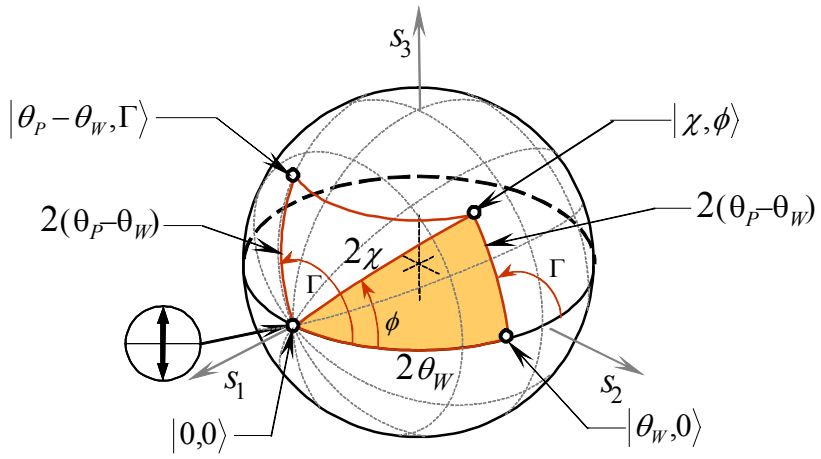

Figure 2.12. Geometric interpretation of the parameters of an off-axis PSG and the parameters of the polarization state generated by it.

The state, $|\theta_P-\theta_W,\Gamma\rangle$ is represented by the point whose polar angle is given by $2(\theta_P-\theta_W)$ from the $|0,0\rangle$ state and whose orientation angle is Γ. That is, $|\theta_P-\theta_W,\Gamma\rangle$ is over the maximum circle that contains the $|0,0\rangle$ state, and is at an angle Γ to the

equator of linear states. And the geodesic distance between $|\theta_P-\theta_W,\Gamma\rangle$ and $|0,0\rangle$ is $2(\theta_P-\theta_W)$. The rotation $\mathbf{R}(\theta_W)$, applied to $|\theta_P-\theta_W,\Gamma\rangle$, produces the state $|\chi,\phi\rangle$. The rotation is represented on Poincaré's sphere by a displacement parallel to the equator of the state, the measure of that rotation is given by an arc of the equator with length $2\theta_W$.

This way, the polarization states $|0,0\rangle$,$|\theta_P-\theta_W,\Gamma\rangle$, and $|\chi,\phi\rangle$ determine a triangle on Poincaré's sphere. We have represented in Figure 2.12, this triangle. However, the arc from the state $|\theta_P-\theta_W,\Gamma\rangle$ to the state $|\chi,\phi\rangle$ is not an arc of maximum circle, therefore it is convenient to use the spherical triangle with vertices $|0,0\rangle$,$|\theta_W,0\rangle$, and $|\chi,\phi\rangle$. In this case the sides are arcs of maximum circle, and therefore, given a polarization state $|\chi,\phi\rangle$, and fixed one of the system parameters, the other parameters can be solved by using simple spherical trigonometry relations.

We will see in the next Section how to use the representation of polarization states and polarizing elements on Poincaré's sphere to determine the relations between the configuration parameters of the PSG (or PSD), and the polarization state generated (or detected) by it.

2.4.5. *Fixed retardance plate solutions*

While the polarization state is determined by two parameters, the PSG or PSD systems, are determined by three parameters, (the angles of the polarizer and retarder plate with respect to the laboratory *x* axis, and the retardance of the retarder plate),

therefore it is necessary to fix one of the parameters of the PSD (or PSD) to have a determined solution. We consider in this section the case in which the retardance of the reterder plate is fixed because usually, an arbitrary(or variable) retardance plate is not available in the laboratory, especially when a large aperture is needed. Therefore, it is necessary to determine whether it is possible or not to generate a given polarization state using a given retarder plate, and to find the parameters of the setup that produce that polarization state as a function of the retardance (Γ) of the available plate. In this case, by solving the spherical triangle, shadowed in Figure 2.12, one finds that the orientation of the linear polarizer and the wave plate are given by the following equations:

$$\sin 2(\theta_P - \theta_W) = \frac{\sin\phi \sin 2\chi}{\sin\Gamma} = \frac{\sin 2\varepsilon}{\sin\Gamma}. \qquad (2.30)$$

and

$$\tan\theta_W = -\frac{\cos\left[\frac{1}{2}(\phi - \Gamma)\right]}{\cos\left[\frac{1}{2}(\phi + \Gamma)\right]} \tan(\theta_P - \theta_W). \qquad (2.31)$$

Equation 2.30 gives the angle between the linear polarizer and the slow axis of the wave plate as a function of the ellipticity of the state $|\chi,\phi\rangle$ and the retardance Γ of the retarder plate. The angle θ_W of the retarder plate to the laboratory x axis is then determined by the solution of equation 2.31. We have seen that the polarization state $|\chi,\phi\rangle$ represented (Figure 2.12) along the maximum circle defined by $|\theta_W,0\rangle$ and $|\chi,\phi\rangle$ is given by

$\mathbf{R}(\theta_W)|\theta_P-\theta_W,\Gamma\rangle$ (the right hand side of equation 2.29). Then, the triangles that are solution for equations 2.30 and 2.31 determine the angles that give the solution for equation 2.29.

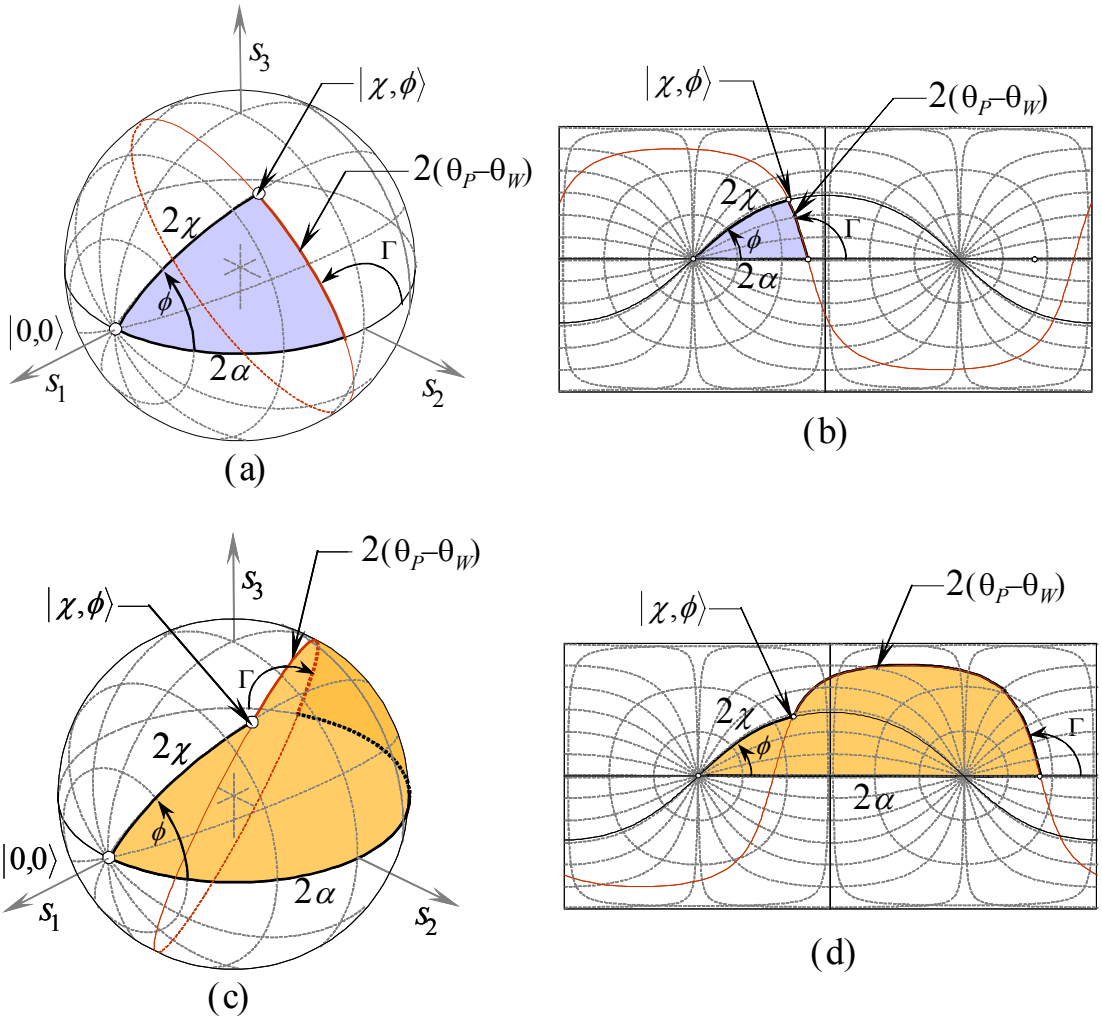

Figure 2.13. Representation on Poincaré's sphere of two configurations of PSG that generate a given polarization state. (a) and (c) represent the triangles on the sphere. (b) and (d) are the corresponding representations of the triangles on a mapping of Poincaré's sphere.

Depending on the value of the quotient in equation 2.30, we can distinguish three cases: when there are two solutions, when there is only one solution and finally when there is not any solution. If the absolute value of the quotient is less than 1,

there are two different solutions for $\theta_P - \theta_W$ in the range between 0 and $\pi/2$. These two solutions lead to two different solutions for θ_P, and θ_W in equations 2.31 that is, one for each solution of $\theta_P - \theta_W$ (θ_W can take values between 0 and π). These solutions correspond to two valid configurations of the setup that reach the same polarization state. The two solutions are represented by the spherical triangles on Poicaré's sphere shown in Figure 2.13. There, we have provided representations of the solution triangles both in the sphere (Figure 2.13a and c) and in a mapping of the sphere (Figure 2.13b and d), in which all the points of the sphere can be represented at once. Let us note that there are two maximum circles (represented in red in Figure 2.13) at an angle Γ to the equator that cross on the point that represents the polarization state $|\chi,\phi\rangle$. Therefore there are two different triangles (The blue and orange triangles in Figure 2.13) that are solution of the system, and there are two solutions for the PSG configuration.

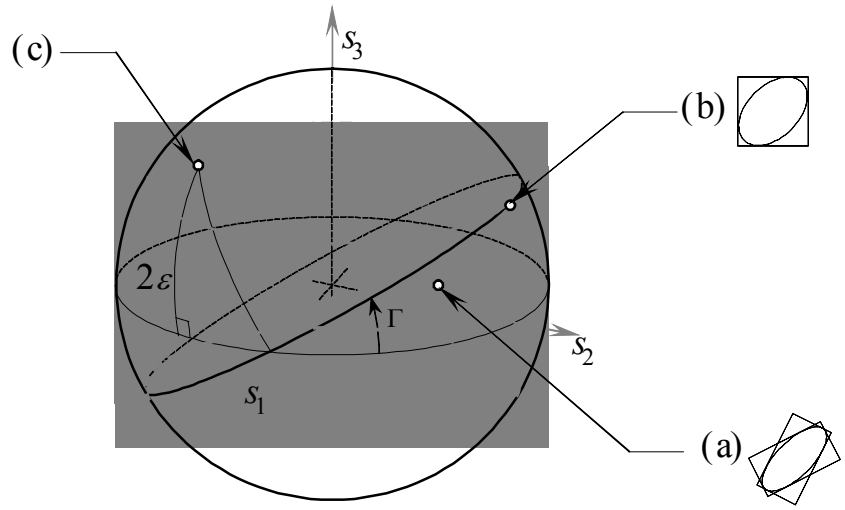

Figure 2.14. Representation in Poincaré's sphere of the polarization states reachable by a PSG composed by a linear polarizer and a Γ-retardance wave plate. The point (a) represents a polarization state that can be obtained by two different configurations using the same retarder plate. Point (b) represents a state that can be generated by a unique configuration. Point (c) represents a polarization state that can not be generated by a PSG that uses a Γ-retardance retarder plate.

The solution for the system is unique when the retardance of the retarder plate is equal to the double-ellipticity angle (2ε) of the polarization state to generate. In this case equation 2.30 leads to $\theta_P - \theta_W = \pi/4$.

Finally, when the double ellipticity angle of the polarization state is bigger than the retardance of the retarder plate, equation 2.30 has no solution because the quotient at the right hand side is bigger than one. That means that the ellipticity of the state can not be reached using this retarder plate.

These three cases are illustrated in Figure 2.14. We represent Poincaré's sphere and the maximum circle corresponding to a Γ-retardance plate. All the states reachable by rotations of this circle about the s_3-axis (corresponding to different orientations

of the retarder plate) have been shadowed. These states define a band whose s_3 coordinate is between $-\sin\Gamma$ and $\sin\Gamma$. So, a given state can be generated by a PSG composed of a linear polarizer and a retarder plate if the representation of the state in Poincaré's sphere is placed on the band defined by the retarder plate. In particular, a quarter-wave plate can reach any polarization state, although a smaller retardance is enough for most of the polarization states needed when working with TLNCs. Let us say, a given polarization state can be generated or detected using any retarder plate whose retardance value is closer to $\pi/2$ than the ellipticity (2ε) of the polarization state. This way the case (a) in Figure 2.14 corresponds to a polarization state that can be reached by two different configurations of a PSG with a Γ-retardance plate. The point in (b) in Figure 2.14 represents a polarization state whose solution is unique for the Γ-retardance plate. Finally the point (c) in Figure 2.14 represents a state that can not be reached by a Γ-retardance plate.

2.4.6. *Relation between PSG and PSD*

The above explained calculi describe how to find the orientations θ_P and θ_W of the polarizing elements in a PSG that generates a polarization state $|\chi,\phi\rangle$. These calculi are also valid to determine the configuration of the PSD that detects the polarization state $|\chi,\phi\rangle$, by establishing the relation between the configurations of the PSD and PSG for a polarization state.

For this, we consider that the PSD transmits completely the polarization state $|\chi,\phi\rangle$ generated by the corresponding PSG. We have represented this in Figure 2.15. We have represented a PSG that generates a polarization state $|\chi,\phi\rangle$, followed by the PSD that detects the same polarization state. For both the PSG and PSD we use retarder plates with retardance $\Gamma_G=\Gamma_D=\Gamma$.

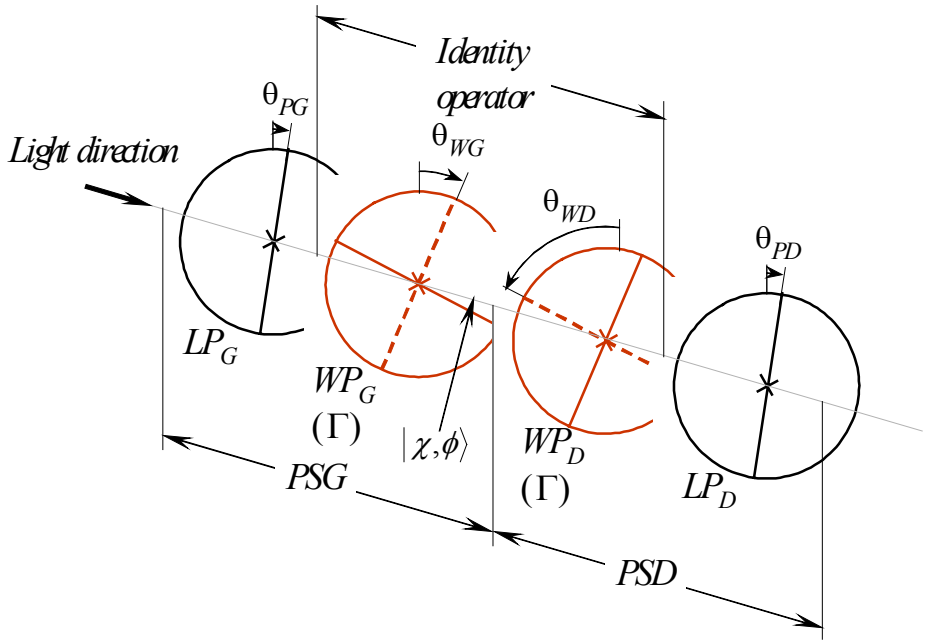

Figure 2.15. Scheme of a PSG followed by a PSD for a polarization state $|\chi,\phi\rangle$. The two retarder plates have equal retardance, but their slow and fast axes are swapped each other.

The condition for the PSD to transmit completely the polarization state $|\chi,\phi\rangle$ is that the polarization state in front of the linear polarizer LP_D (see Figure 2.15)is a linear polarization state. This can be achieved if the phase delay between linear components, introduced by the first retarder plate WP_G is compensated by the second retarder WP_G plate. Considering that the retardance for both retarder plates is Γ, the phase delay is compensated when the slow axis of WP_D is parallel to the fast

axis of WP_G. That is, when $\theta_{WD}=\theta_{WG}+\pi/2$ rad. In this case, the polarization state in front of LP_D is the same linear polarization state generated after the first polarizer LP_G. Therefore, to obtain full transmission, the orientation of the polarization state detector is $\theta_{PD}=\theta_{PG}$.

Summarizing, the relation between the configuration of a PSG and a PSD corresponding to a given polarization state, and considering the same retarder plate is given by

$$\begin{aligned} &\theta_{PD} = \theta_{PG} \\ &\theta_{WD} = \theta_{WG} + \pi/2 . \\ &\Gamma_D = \Gamma_G \end{aligned} \tag{2.32}$$

2.5.The modulation of liquid crystal panels

In this section we apply the relation established between the PSG and PSD systems and the generated and detected states to develop a compact equation for the amplitude and phase modulation of the spatial light modulator and we introduce the TNLC panel by an operator as a function of the free parameters that determine the polarization state.

2.5.1. *General modulation function*

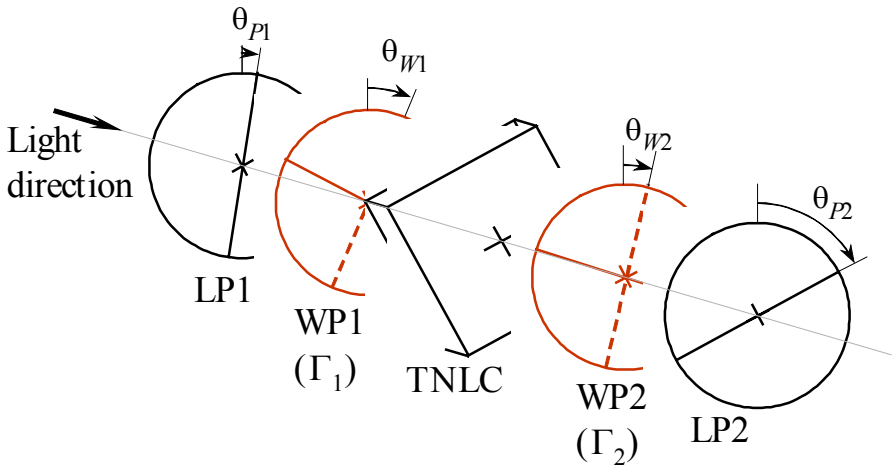

Figure 2.16. Scheme of the spatial light modulator based on elliptic light modulation by a TNLC.

The studied spatial light modulator system based on elliptic polarization modulation is composed by a liquid crystal panel placed between two linear polarizers (LP1 and LP2 in Figure 2.16) and two retarder plates (WP1 and WP2 in Figure 2.16). The behavior of the complete system is described by a Jones operator $\mathbf{M}_{SLM}$ that can be obtained by composing the operators for the different elements in the system. Therefore we have

$$\mathbf{M}_{SLM} = \mathbf{P}(\theta_{P2})\mathbf{W}(\Gamma_2,\theta_{W2})\mathbf{U}_{LC}(V)\mathbf{W}(\Gamma_1,\theta_{W1})\mathbf{P}(\theta_{P1}). \qquad (2.33)$$

Here $\mathbf{U}_{LC}(V)$ is the Jones operator that describes the polarization characteristics of the liquid crystal panel as a function of the applied voltage. This matrix, $\mathbf{U}_{LC}(V)$, will be described in Sections 2.5.2 to 2.5.6. $\mathbf{P}(\theta_{P1})$ and $\mathbf{P}(\theta_{P2})$ are the operators corresponding to the input and output polarizers, respectively, and $\mathbf{W}(\Gamma_1,\theta_{W1})$ and $\mathbf{W}(\Gamma_2,\theta_{W2})$ are the operators for

the retarder plates. The angles of these elements are represented in Figure 2.16.

We have demonstrated in Section 2.4 that the association of a linear polarizer with a retarder plate constitutes a polarization state generator (PSG), and that the same elements in inverse order constitute a polarization state detector (PSD). This way we can write $\mathbf{M}_{SLM}$ as follows:

$$\mathbf{M}_{SLM} = |\theta_{P2}\rangle\langle out|\mathbf{U}_{LC}(V)|in\rangle\langle\theta_{P1}| . \tag{2.34}$$

Here $|in\rangle$ is the state generated by the PSG, and $|out\rangle$ is the polarization state detected by the PSD. They are given by

$$\begin{cases} |in\rangle = |\chi_1, \phi_1\rangle = \mathbf{R}(\theta_{W1})|\theta_{P1} - \theta_{W1}, \Gamma_1\rangle \\ |out\rangle = |\chi_2, \phi_2\rangle = \mathbf{R}(\theta_{W2})|\theta_{P2} - \theta_{W2}, -\Gamma_2\rangle \end{cases} . \tag{2.35}$$

This way, when the system is illuminated by an arbitrary polarization state, $|A\rangle$, the following polarization state is obtained at the output of the optical system :

$$\mathbf{M}_{SLM}|A\rangle = |\theta_{P2}\rangle\langle out|\mathbf{U}_{LC}(V)|in\rangle\langle\theta_{P1}|A\rangle . \tag{2.36}$$

Of course, this is a linear polarization state along the direction of the output polarizer. The amplitude and phase of the wave is determined by the scalar factors that multiply the unit vector $|\theta_{P2}\rangle$. Note that $\langle\theta_{P1}|A\rangle$ represents the amplitude and phase after the first polarizer; because the intensity at this point is the maximum intensity that can be reached after the SLM system, we take it as the reference, and we use it as a normalization

factor. We can do so because $\langle \theta_{P1} | A \rangle$ is independent of the voltage applied to the liquid crystal.

This way the modulation of the SLM is given by the following complex valued function $\mu(V;\chi_1,\phi_1,\chi_2,\phi_2)=T(V)\exp i\tau(V)$.

$$\mu(V;\chi_1,\phi_1,\chi_2,\phi_2) = \langle out | \mathbf{U}_{LC}(V) | in \rangle . \qquad (2.37)$$

The transmittance is the magnitude of $\mu(V;\chi_1,\phi_1,\chi_2,\phi_2)$, that we call $T(V)$ and the phase modulation is given by its argument, $\tau(V)$.

Note that, once the explicit dependence on V of the TNLC panel is defined, the operation curve of the system depends only on the four parameters of the generated and detected states.

2.5.2. *Jones operator for TNLCs*

The polarization characteristics of TNLC panels are given by the structured orientation of the molecules of the liquid crystal that compose it and by the possibility of changing this structure by applying an external electric field. Because we consider uniaxial materials, the orientation of the molecules is determined by two angles, the tilt angle and the twist angle, represented in Figure 2.17.

Both the twist angle and the tilt angle of the molecules can be modified by an external electric field. For light with normal incidence to the TNLC panel, variations of the tilt angle are translated into variations of the effective birefringence of the

material. That is for low tilt angles the birefringence is close to the intrinsic birefringence of the material and for big tilt angles there is no birefringence because the electromagnetic field is perpendicular to the revolution axis of the index ellipsoid.

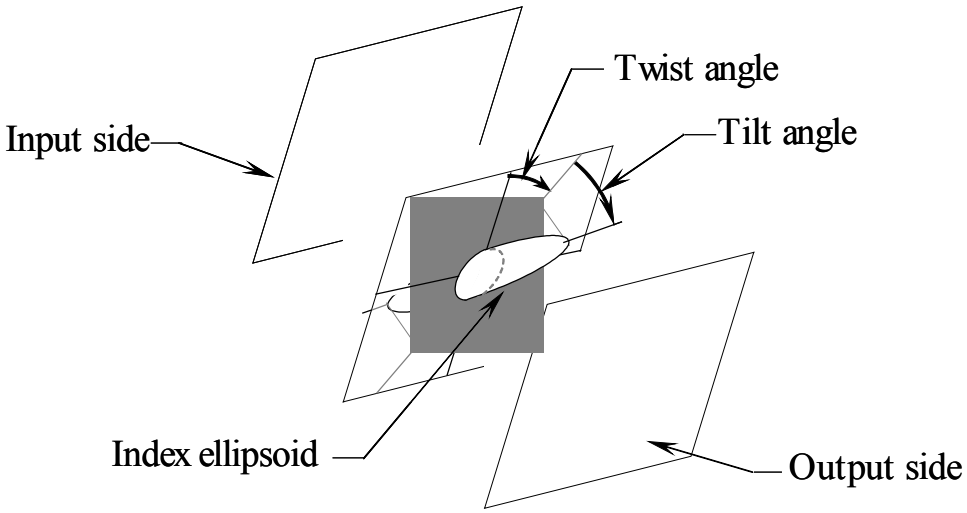

Figure 2.17. Angles that characterize the orientation of a uniaxial birefringent molecule.

In the case of nematic liquid crystals, the molecules are disposed in layers: that is, all the molecules in the same layer have the same orientation. In addition, for twisted nematic liquid crystals, the twist of each layer is slightly rotated with respect to the previous layer. This is represented in Figure 2.18. This way, each layer behaves like an extremely thin retarder plate, whose orientation and birefringence are related with the twist and the tilt angle. respectively.

This way, the Jones matrix for a TNLC is the limit when the number of layers is infinite (and their thickness is zero) of the composition of the matrices for the corresponding retarder

plates, whose birefringence and orientation depend on the depth of the layer.

The dependence of the tilt and twist angle (that determine the birefringence and orientation of the composed retarder plates) is determined by the chemical composition of the liquid crystal and the manufacturing process. However, these details are not usually available, therefore it becomes necessary to approximate the tilt and twist variations as a function of few parameters that can be directly measured, for the understanding of the liquid crystal panel.

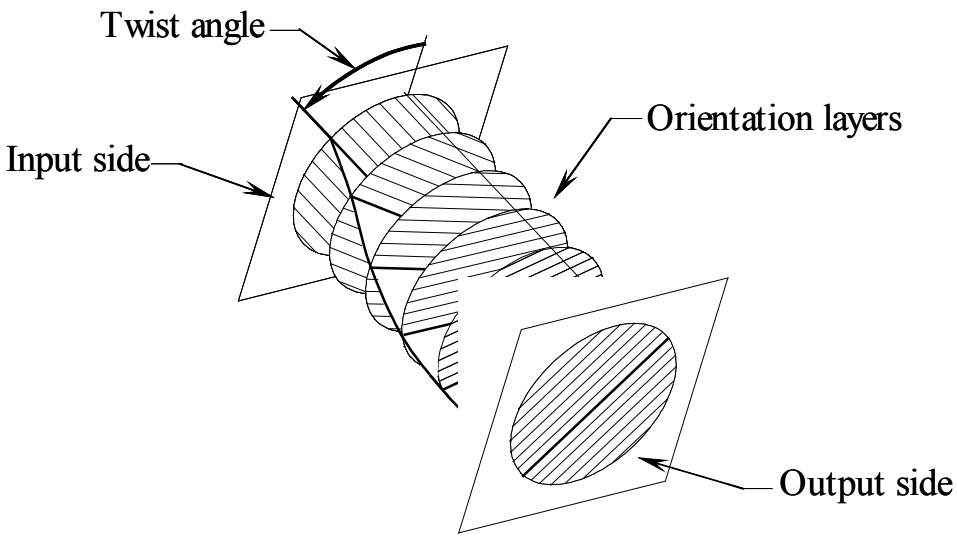

Figure 2.18. Scheme of the orientation of the molecules in a twisted nematic liquid crystal.

2.5.3. *Lu and Saleh model*

Lu and Saleh **[Lu90]** proposed and developed the first simple Jones matrix model for TNLCs. This model considers that the twist angle increases linearly with the depth of the layer, independently of the applied voltage (see Figure 2.19a). This

way it can be characterized by two simple parameters, such as the orientation of the molecules at the input side, Ψ_D (input director axis) and the twist difference between the two sides of the TNLC, α.

In the Lu and Saleh model the tilt angle of the molecules (Figure 2.19b), and therefore the birefringence of the layers is uniform along the depth of the panel. The value of this uniform angle depends on the applied voltage. This way, when there is no voltage the molecules are oriented parallel to the sides of the TNLC panel and for a given voltage V_{max} they get aligned perpendicularly to the sides (input and output).

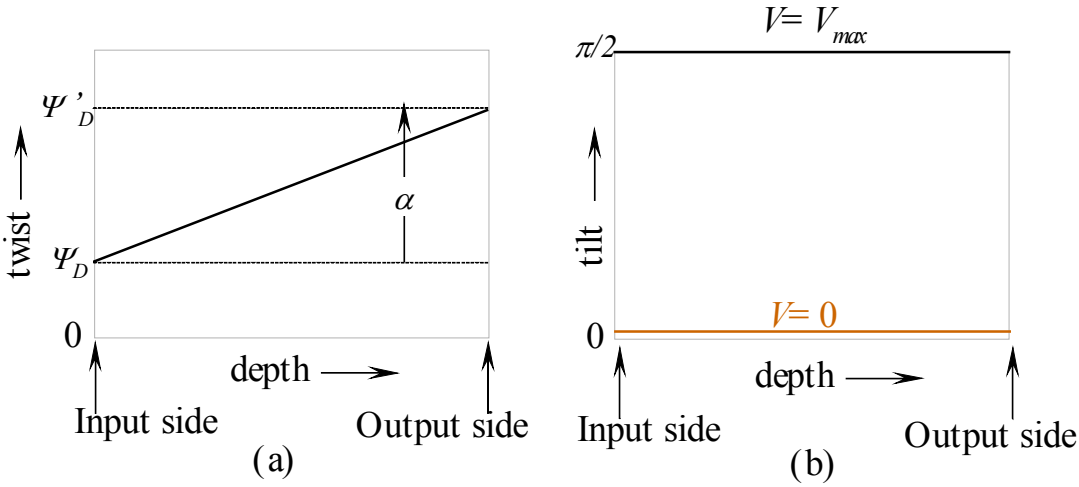

Figure 2.19. Twist and tilt angles for the Lu and Saleh model of TNLC.

However because the intrinsic birefringence of the material is usually unknown, instead of describing the tilt angle for a given value of V, one characterizes a birefringence parameter $\beta(V)$, which represents the effective birefringence for normal

incidence light, and that is determined by the tilt angle of the molecules, according to next expressions:

$$\beta(V) = \frac{2\pi}{\lambda}[n(V) - n_o]d. \tag{2.38}$$

where λ is the wavelength of light, d is the thickness of the panel n_o is the ordinary index of the material and $n(V)$ is given by

$$\frac{1}{n^2(V)} = \frac{\sin^2[\theta(V)]}{n_o^2} + \frac{\cos^2[\theta(V)]}{n_e^2}, \tag{2.39}$$

where $\theta(V)$ is the tilt angle for an external voltage V..

Lu and Saleh **[Lu90]**, demonstrated that the corresponding Jones matrix $\mathbf{U}_{LU}$, can be written as a function of the parameters (Ψ_D, α and $\beta(V)$) that characterize the model, as follows.

$$\mathbf{U}_{LU} = \exp i\beta \cdot \mathbf{R}(-\alpha) \cdot \mathbf{M}(\alpha, \beta). \tag{2.40}$$

where $\mathbf{R}(-\alpha)$ is the rotation matrix and $\mathbf{M}(\alpha,\beta)$ is a unitary matrix that can be written as follows.

$$\mathbf{M} = \begin{bmatrix} X - iY & Z \\ -Z & X + iY \end{bmatrix}. \tag{2.41}$$

where

$$X = \cos\gamma, \tag{2.42a}$$

$$Y = \frac{\beta}{\gamma}\sin\gamma, \tag{2.42b}$$

$$Z = \frac{\alpha}{\gamma}\sin\gamma\,, \qquad (2.42c)$$

and

$$\gamma = +\sqrt{\alpha^2 + \beta^2}\,. \qquad (2.42d)$$

These expressions are referred to the frame determined by the director axis at the input side of the TNLC, which is at an angle Ψ_D to the *x*-axis of the laboratory frame. This way, to characterize the behavior of a TNLC panel, the only parameters that have to be measured are,

a) The orientation of the director axis at the input side (Ψ_D).

b) The twist angle (α).

c) The birefringence as a function of the applied voltage. ($\beta(V)$)

The techniques to measure these parameters are given in Refs. **[Soutar94]** **[Davis99B]** **[Davis99D]**. They consist on fitting the theoretical prediction for some intensity transmission curves to the experimental ones.

2.5.4. *Coy et al model.*

The model proposed by Lu and Saleh was first modified by Coy *et al* **[Coy96]** and later by Márquez *et al* **[Márquez2000]**

The Coy *et al* model consists on considering that there exist two outer layers at the input side and the output side of the TNLC that do not twist. This way, they consider the twist angle variation as shown in Figure 2.20a. The modulator can be thought as divided in three parts, the two outer layers and the

inner layer. The outer layers have fixed thickness d_e, and they behave as regular retarder plates because in these layers the molecules are not twisted. Therefore a new parameter δ, corresponding to the birefringence of these layers is introduced in the Coy *et al* model.

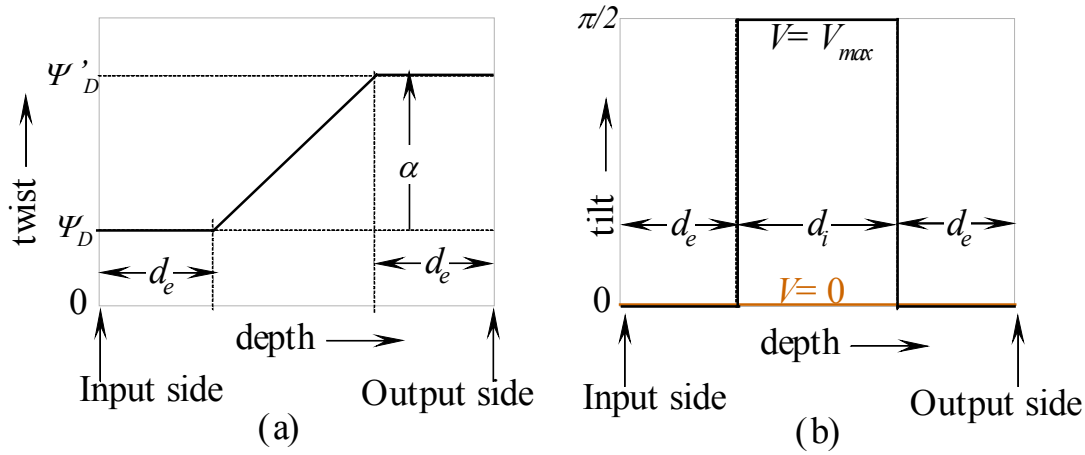

Figure 2.20. Coy model approximation for the twist and tilt angle. (a) twist angle *vs* depth, (b) tilt angle *vs* depth.

In the inner layer, the twist is considered to be a linear function of the depth (Figure 2.20a), and the tilt angle is considered to be constant, but with a value different to the outer layers, as represented in Figure 2.20b.

Therefore, the Jones matrix for a TNLC predicted by the Coy model, can be obtained by composing the Lu and Saleh matrix for the inner layer with two retarder plate matrices for the outer layers. Then, the resulting matrix can be written as

$$\mathbf{U}_{COY} = \exp i(\beta+\delta)\cdot\mathbf{R}(-\alpha)\begin{bmatrix} X'-iY' & Z \\ -Z & X'+iY' \end{bmatrix}, \qquad (2.43)$$

where

$$X' = X\cos\delta - Y\sin\delta \,. \qquad (2.44a)$$

$$Y' = X\sin\delta + Y\cos\delta \,. \qquad (2.44b)$$

2.5.5. *Márquez et al model*

A further modification of the Coy *et al* model for TNLCs was proposed by Márquez *et al* **[Márquez2000]**. The authors consider that the effect of the outer layers depends on the applied voltage, that is, they consider that the thickness of the layers of molecules that do not twist is affected by the applied voltage. The corresponding approximations for the twist and tilt angle are represented in Figure 2.21a and b, respectively. The red traces represent the twist and tilt dependence on the depth of the TNLC cell when the applied voltage is almost zero. In this case the edge layers are very thin. One can observe that in the range of low voltage, the Márquez *et al* model approximates the Lu and Saleh model. The black traces in Figure 2.21 represent the twist and tilt when the applied voltage is the saturation voltage (V_{max}). In this range (near the saturation voltage) the Márquez *et al* model approximates the Coy *et al* model.

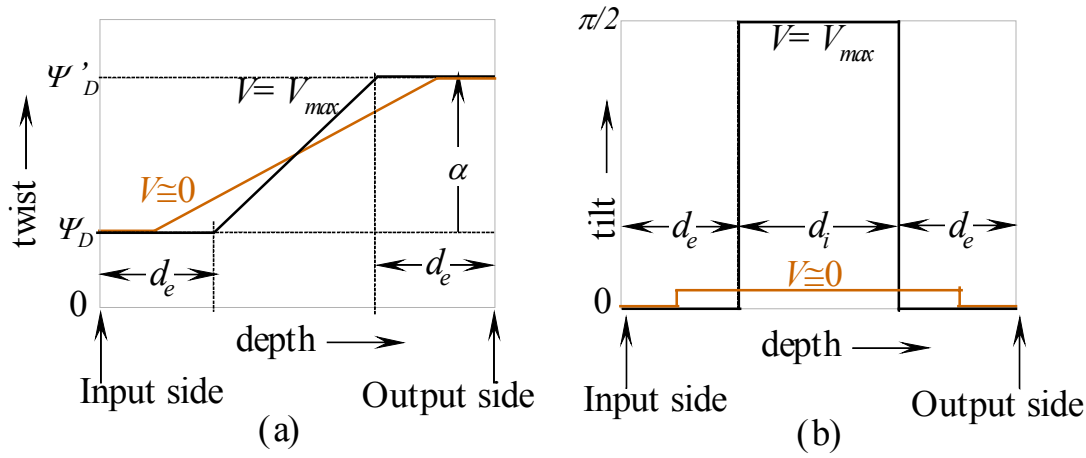

Figure 2.21. Twist and tilt angle for the Márquez *et al* model. (a) twist angle for values of the applied voltage (in red and in black). (b) tilt angle for the corresponding values of the applied voltage.

The Jones operator corresponding to the Márquez *et al* model can be represented by the same matrix as for the Coy *et al* model (equations 2.43 and 2.44). However, there is the important difference that in this case the birefringence parameter for the edge layers, δ, depends on the external voltage.

This way, the TNLC panel can be completely determined by measuring four parameters:

a) The orientation of the director axis at the input side (Ψ_D).

b) The twist angle α.

c) The birefringence of the inner layer of the TNLC $\beta(V)$, which depends on the voltage.

d) The birefringence of the outer layer $\delta(V)$, which depends on the applied voltage.

2.5.6. *Experimental calibration of the TLNC matrix*

The above described parameters can be measured by experiments of linear polarization states intensity transmission. Experimental transmission results are compared with theoretical predictions, which depend on the unknown parameters. These parameters are fitted by minimizing the squared differences between the theoretical predictions determined by them and the experimental results. The details of the calibration technique are given in **[Soutar94] [Davis99B] [Davis99D] [Márquez2000]**.

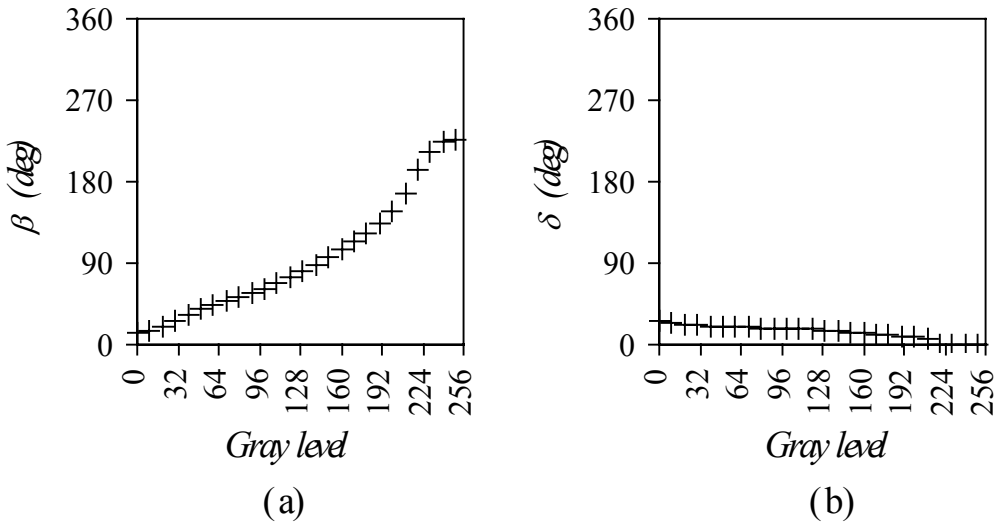

Figure 2.22. Experimental birefringence of the Sony-Red-0 panel for a wavelength λ=457nm. (a) β(V) *vs* gray level. (b) δ(V) *vs* gray level.

In our correlator we use two TNLCs panels, model SONY LCX012AL, with VGA resolution. We tab as **Sony-red-0** the panel used in the correlator scene. And **Sony-red-1** is the tab for the panel used in the filter.

The orientation of the director axis and the twist angle for the panel tabbed as Sony-Red-0 are

$$\alpha = -91.8\text{deg},$$

$$\Psi_D = 46.2 \text{ deg}$$

respectively, and the birefringences $\beta(V)$ and $\delta(V)$ for light with wavelength λ=457nm are represented in Figure 2.22a and b respectively, as functions of the gray level signal sent to the LCD controller. One can observe in Figure 2.22a that the maximum birefringence ($\beta(V)$), that is the total phase difference between orthogonal polarization components does not reach the 2π phase.

For the panel used in the filter SLM of the correlator, tabbed as Sony-Red-1, the parameters are:

$$\alpha = -91.9 \text{ deg},$$

$$\Psi_D = 44.9 \text{ deg}$$

And the birefringences $\beta(V)$ and $\delta(V)$ are those represented in Figure 2.23a and b respectively.

The response is quite similar to that of the scene panel. In this case the birefringence is also lower than 2π radians (see Figure 2.23a).

These parameters fully characterize the TNLC panels used in the SLM system. In addition the model is accurate enough for any kind of polarization configuration used at the input and output of the panels **[Márquez2001A].** Therefore, it can be

used for the optimization processes that are described in next sections.

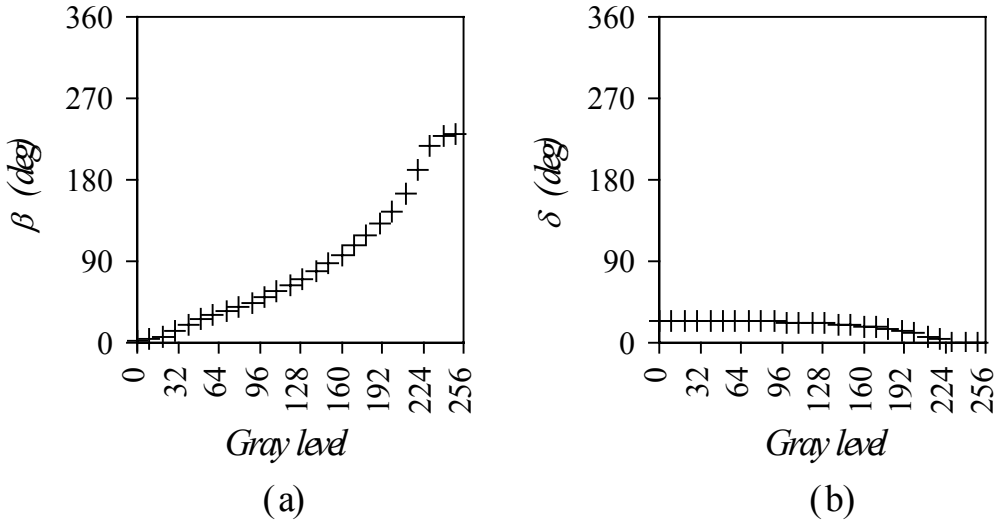

Figure 2.23. Experimental birefringence of the Sony-Red-1 panel for wavelength λ=457nm. (a) $\beta(V)$ *vs* gray level. (b) $\delta(V)$ *vs* gray level.

2.6.Amplitude only modulation

In this section we explain the method we propose for the optimization of the TNLC-based SLMs for amplitude only modulation regime. The modulation expression of the elliptic light modulation system is given by equation 2.37. Aside from the polarization states, it depends on the operator that describes the TNLC. For this, we consider the operator corresponding to the Márquez *et al* model of TNLC, described in Section 2.5.5. Then, the modulation can be written in terms of the four parameters that determine the input and output states and we can proceed to optimize the response of the SLM system.

2.6.1. *The quality criterion*

The criterion to evaluate the quality of a modulation response as amplitude only modulation , considers the following aspects:

a) Minimum phase variation.

b) Maximum dynamic range for the transmittance.

c) Maximum contrast of the transmittance.

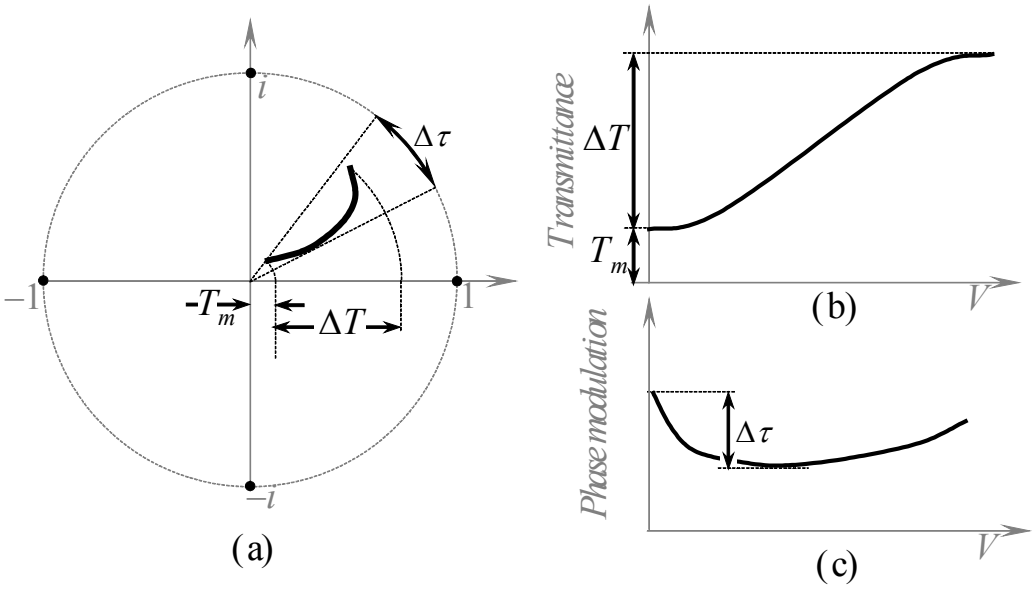

Figure 2.24. Scheme of the parameters involved in the merit function for amplitude only modulation. (a) Operation curve on the complex plane. (b) Transmittance versus applied voltage. (c) Phase modulation versus applied voltage.

Each one of these aspects is quantified by a term of the merit function. In Figure 2.24 we represent an example of operation curve in order to clarify in the figure the parameters that appear in the merit function. This way the flatness of the phase response is represented by the difference between the maximum and minimum phase modulation introduced by the

system, represented in Figure 2.24a and c by $\Delta\tau$. The dynamic range is the difference between the maximum and the minimum transmittances, it is represented by ΔT in Figure 2.24a and b. A normalized measure of the amplitude contrast is given by the ratio between the dynamic range, ΔT, and the maximum transmittance. $T_m+\Delta T$. To maximize the contrast is equivalent to minimize T_m for a given ΔT (see Figure 2.24a and b). This is important to avoid the presence of a non null background in the input SLM of the real time correlator, that may produce interferences on the correlation plane.

Therefore, we can define the following quality criterion Q_{AO},:

$$Q_{AO}[\mu(V)] = \frac{1}{\lambda_1+\lambda_2+\lambda_3}\left[\lambda_1\left(1-\frac{\Delta\tau}{2\pi}\right)+\lambda_2\Delta T+\lambda_3\frac{\Delta T}{\Delta T+T_m}\right]. \qquad (2.45)$$

Here $\lambda_1,\lambda_2,\lambda_3$ are coefficients used to weight the importance of each one of the conditions in the optimization process, and to normalize the function between zero and one. Note that, aside from the weight coefficients, the optimal value for each term is one, considering that the maximum transmittance is one and the maximum phase range is 2π. Therefore, Q_{AO} is 1 only for a perfect amplitude only modulation response.

Each one of the terms that take part in the quality criterion can be written as a function of the modulation function $\mu(V)$ as follows:

$$T_m = \min_V \sqrt{\mu^*(V)\mu(V)}\,, \tag{2.46a}$$

$$\Delta\tau = \max_V \left\{ \tan^{-1}\left[i\frac{\mu^*(V)-\mu(V)}{\mu^*(V)+\mu(V)} \right] \right\} - \min_V \left\{ \tan^{-1}\left[i\frac{\mu^*(V)-\mu(V)}{\mu^*(V)+\mu(V)} \right] \right\}, \tag{2.46b}$$

and

$$\Delta T = \max_V \sqrt{\mu^*(V)\mu(V)} - T_m\,. \tag{2.46c}$$

Therefore, $Q_{AO}[\mu(V)]$ is a function of the parameters of $\mu(V)$, that is, a function of the parameters that define the input and output polarization states, χ_1,ϕ_1,χ_2 and ϕ_2 in equation 2.37, aside from the parameters of the physical model for the TNLC.

2.6.2. *Optimization algorithm.*

Although the merit function depends on the parameters that define the generated and detected polarization state, its explicit dependence on the parameters χ_1, ϕ_1, χ_2, and ϕ_2 is not an analytical function, and the maximization must be performed numerically.

The algorithm we have programmed for the numerical optimization of the quality criterion function is based on the conjugate gradient method. In this method the maxima are approximated by successive iterations. At each iteration the gradient of the function is evaluated for a given set of parameters. The gradient indicates the direction (in the parameters space), in which the function presents maximum slope. The method consists of taking a new point (that is, a new set of values for the parameters) on the maximal slope direction for the subsequent iteration.

The solutions obtained using the conjugate gradient method (or other derivative-based methods) are local maxima of the quality function. However, $Q_{AO}(\chi_1,\phi_1,\chi_2,\phi_2)$ may have some local maxima that are not the absolute maximum. This must be taken into account in the optimization algorithm.

The algorithm we have programmed for the optimization of the quality function is outlined in Figure 2.25. The principle of the algorithm is to perturb the solution provided by the gradient conjugate method and use it as the starting point for a new optimization. This way, a new solution is obtained and it is compared with the previous one. The best of the two solutions is used for the next iteration. The algorithm finishes when the same solution is the best one after a preset number of iterations.

This way, if the conjugate gradient optimization leads to a local minimum, the perturbation of the solution may produce a new starting point that leads to a different maximum. If the solution is the absolute maximum, there is no possibility of obtaining a better solution, and the algorithm finishes after a fixed number of attempts.

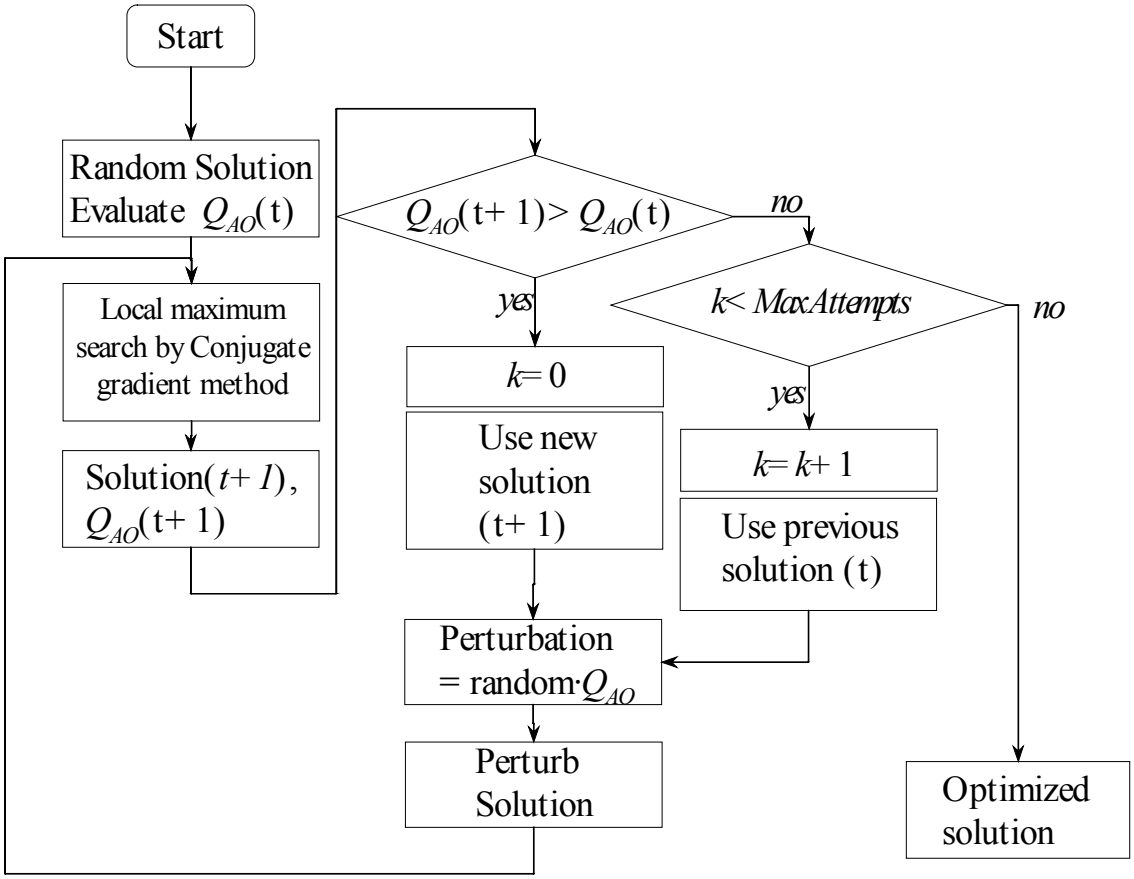

Figure 2.25. Flow diagram of the algorithm programmed for the optimization of the quality criterion.

Let us remark that the variance of the perturbation applied to each solution is inversely proportional to the value of the quality function at that solution. This way, good results are slightly perturbed, and bad results are strongly perturbed.

2.6.3. *Optimization results.*

The proposed algorithm has been applied to obtain an amplitude only response configuration for the TNLC-based spatial light modulator used in the scene of the correlator. We have used the panel tabbed as Sony-Red-0. The corresponding

parameters that characterize this panel according to the Márquez *et al* model are given in section 2.5.6.

For the optimization of the amplitude only modulation we have used the merit function given in equation 2.45 using the following weight constants: λ_1=10, λ_2=1, λ_3=10. This way, the most important terms are the phase modulation term and the contrast term.

The parameters of the optimal solution provided by the optimization method, and the value of the quality function (normalized to 100) are given in Table 2.2. The parameters are the angles, χ_1, and χ_2, and the phase delay between components, ϕ_1, and ϕ_2, of the generated and detected polarization states, expressed in the frame determined by the input director axis of the TNLC.

χ_1(deg)	ϕ_1(deg)	χ_2(deg)	ϕ_2(deg)	100× Q_{AO}
29.2	39.5	37.6	136.4	93.91

Table 2.2. Parameters of the optimal solution for amplitude only modulation response.

The value of the merit function Q_{AO} provided by the obtained configuration is the 93.91% of the value of the merit function for the perfect amplitude only modulation. This represents a very good result, and allows us to use the TNLC-based SLM in amplitude only modulation regime.

The transmittance and the phase modulation predicted for this configuration are represented as a function of the gray level

signal in Figure 2.26a and b respectively. One can observe an almost flat phase response, and a quite wide dynamic range for the transmission, with very good contrast.

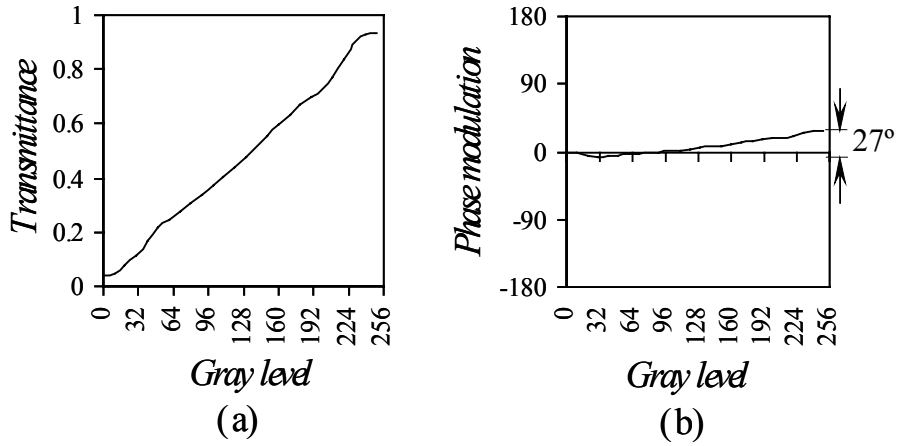

Figure 2.26. (a) Transmittance and (b) phase modulation response for the optimal amplitude only configuration as a function of the gray level .

2.6.4. *The implementation using arbitrary plates*

Once the generated and detected polarization states are found it is possible to determine the configuration of the corresponding PSG and PSD. To determine the minimum retardance to be used, we consider the double of the ellipticity angle ε (see equation 2.16) for the polarization states. That is:

$$2\varepsilon_1 = +33.2 \text{ deg}$$

for the input polarization state and

$$2\varepsilon_2 = +41.8 \text{ deg}$$

for the output polarization state.

PSG			PSD		
θ_P(deg)	θ_W(deg)	Γ(deg)	θ_P(deg)	θ_W(deg)	Γ(deg)
161	140	125	16	307	94.5
146	77	125	54	33	94.5

Table 2.3. Orientations of the elements of the PSG and PSD for the amplitude only configuration setup of the spatial light modulator.

This way, according to equation 2.30 one needs a retarder plate with retardance between 33.2 deg and 146.8 deg (=180–33.2) for the PSG, and a retarder with retardance between 41.8 deg and 138.2 deg (=180–41.8) for the PSD. For the PSG we use a 125 deg retardance plate and for the PSD we use a 94.5 deg retardance plate. As explained in Section 2.4.5, these values of the retardance provide two possible configurations for the PSG (and two solutions for the PSD). The configurations of the PSG and PSD are obtained by introducing the parameters of the polarization states χ and ϕ, and the retardances of the retarder plates Γ, in equations 2.30 and 2.31. For the case of the PSD, we have also taken into account the considerations explained in Section 2.4.6. These expressions lead to the orientations of the polarizing elements given in Table 2.3 (right columns of the table).

We have used the configuration in the first row of Table 2.3 for the scene spatial light modulator system. The experimental amplitude and phase modulation, and the theoretical prediction given by the modulation equation 2.37, based on the Márquez *et al.* model, are represented in Figure 2.27a and b respectively, One observes a wide dynamic range, with good contrast in the

amplitude transmission response, and an almost flat phase modulation. Experimental results are in very good accordance to theoretical predictions.

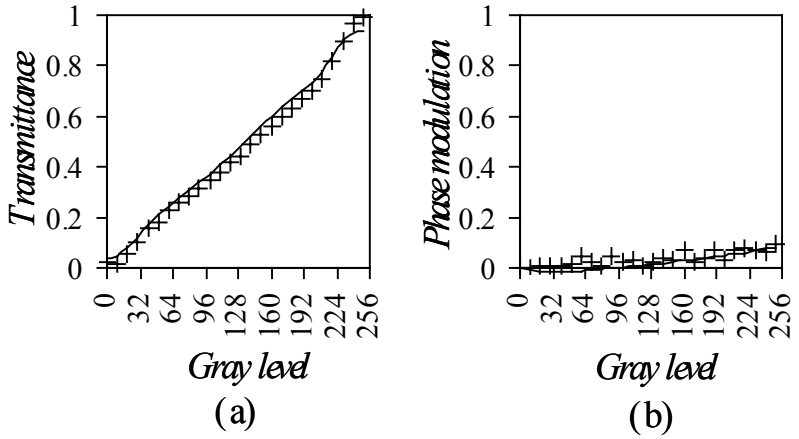

Figure 2.27. Modulation response for the amplitude only configuration of the spatial light modulator The crosses (+) indicate experimental results and solid line represents theoretical prediction. (a) Transmittance. (b) Phase modulation (in 2π units).

2.7.Phase only modulation

The same optimization procedure can be used to obtain a configuration that provides phase only modulation by using a different merit function. In this section we propose a merit function to quantify the quality of an operation curve as a phase only modulation. We use the proposed merit function to obtaion the parameters that determine the optimal polarization states at the input and output of the TNLC panel. Finally, we provide the configuration of the PSG and PSD necessary to generate and detect these states. The obtained phase only modulation configuration will be found for both the scene SLM and the filter SLM.

2.7.1. *The optimization criterion*

The phase only modulation criterion must consider the following aspects:

a) Maximum dynamic range for the phase modulation, if possible from 0 to 2π.

b) Amplitude transmittance as flat as possible.

c) Light efficiency. That is, the transmittance value must be constant but also as high as possible. This can be quantified by the average value, or (in our case) by the minimum value.

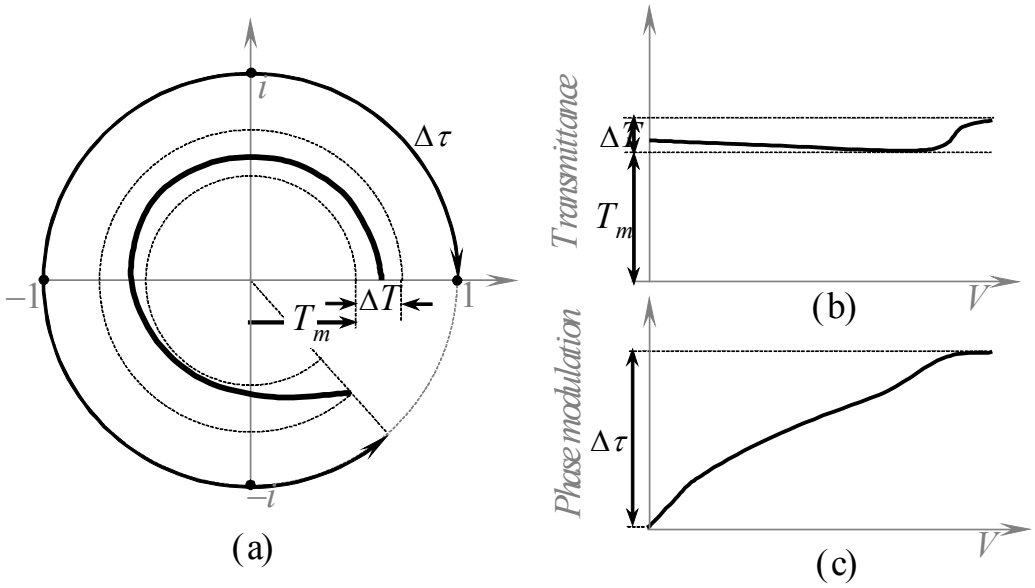

Figure 2.28. Parameters of the modulation that are considered in the phase only modulation quality function. (a) Operation curve in the complex plane (b) Transmittance *vs* applied voltage. (c) Phase modulation *vs* applied voltage.

The dynamic range of the phase modulation is given by the difference between the maximum and the minimum of the argument of the modulation function evaluated in the used voltage range. In Figure 2.28 we represent a given response

curve in order to define the values that appear involved in the merit function. The dynamic range of the phase is represented by $\Delta\tau$ in Figure 2.28a and c. The flatness of the amplitude transmittance is evaluated by considering the amplitude dynamic range, represented as ΔT in Figure 2.28a and b. And the light efficiency is evaluated by considering the minimum value of the transmittance T_m (Figure 2.28a and b). Because the SLM does not amplify the light ΔT and T_m are between 0 and 1.

Therefore, we can define the following quality function Q_{PO}, composed of three terms normalized between 0 and 1, and that express the three mentioned criteria.

$$Q_{PO}[\mu(V)] = \frac{1}{\lambda_1 + \lambda_2 + \lambda_3}\left[\lambda_1 \frac{\Delta\tau}{2\pi} + \lambda_2(1-\Delta T) + \lambda_3 T_m\right]. \qquad (2.47)$$

Analogously to the case of the amplitude only quality function, λ_1, λ_2, λ_3 are coefficients used to weight the importance of each one of the conditions in the optimization process, and to normalize the function between zero and one. In this case, Q_{PO} is 1 only for a perfect phase only modulation response with 2π phase modulation range. The expression of the elements that take part in the quality criterion as functions of the modulation function $\mu(V)$ are given by equations 2.46a, b and c.

This way, $Q_{PO}[\mu(V)]$ depends on χ_1, ϕ_1, χ_2 and ϕ_2. The optimization algorithm described in section 2.6.2 can be applied to find the polarization states that provide the highest value of the merit function Q_{PO} (equation 2.47).

2.7.2. *Results*

The above explained optimization method has been used to obtain the configuration of both the scene and the filter SLMs of the proposed correlator to work in phase only modulation regime. We have used the merit function (Q_{PO}) described in Section 2.7.1, which evaluates the quality of an operation curve as a phase only modulation. We have considered the following values for the normalization coefficients: λ_1=10, λ_2=10, and λ_3=1. This way, we emphasize the importance of the phase modulation dynamic range and of the flatness of the transmittance in front of the light efficiency, which is not so important as the other parameters.

LCD	χ_1(deg)	ϕ_1(deg)	χ_2(deg)	ϕ_2(deg)	100× Q_{PO}
Scene	58.4	133.6	41.6	305.7	97.78
Filter	41.6	49.8	19.1	314.9	94.36

Table 2.4. Optimal set of parameters for the phase only modulation regime of the scene and filter spatial light modulator systems.

The optimization algorithm leads to a set of four parameters χ_1, ϕ_1, χ_2 and ϕ_2, that determine polarization states generated in front of the TNLC and detected behind the TNLC, optimal for the phase only modulation quality criterion. The obtained parameters are detailed in Table 2.4, for both the scene SLM (Sony-Red-0 in Section 2.5.6) and the filter SLM (Sony-Red-1).

One can observe that the values of the quality criterion (100×Q_{PO}) for both the cases of the scene SLM and the filter SLM are quite near to 100. This indicates that, in both cases, the

obtained operation curve, is very close to the operation curve of the perfect phase only modulation.

The ellipticity angle of the polarization states determined by the parameters given in Table 2.4 are

$$2\varepsilon_1 = 40.2 \text{ deg}$$

and

$$2\varepsilon_2 = 49.3 \text{deg}$$

for the scene SLM, and

$$2\varepsilon_1 = -53.7 \text{ deg}$$

and

$$2\varepsilon_2 = -26.0 \text{ deg}$$

for the filter SLM. According to the discussion developed in Section 2.4.5, these ellipticity angles establish the limits for the retardance of the retarder plates used in the PSGs and PSDs.

For the scene SLM we use the same retarder plates as those used for the amplitude only configuration (obtained in Section 2.6), that is $\Gamma_1 = 125\text{deg}$ for the PSG, and $\Gamma_2 = 94.5\text{deg}$, for the PSD. These retardances are within the limits established by the ellipticity angles of the input and output polarization states. The angle configuration for the PSG and PSD for the scene SLM, given by equations 2.30 and 2.31, are detailed in Table 2.5.

For the PSG and PSD of the filter SLM we use retarder plates with retardances $\Gamma_1 = 50\text{deg}$, and $\Gamma_2 = 88.0\text{deg}$, respectively. Note in this case that the retardance for the plate in the PSG is very close to the limit established by the ellipticity angle of the input

polarization state ($2\varepsilon_1$=40.2deg), nevertheless it is adequate to generate the input polarization state. The angle configuration for the PSG and PSD of the filter SLM are also presented in Table 2.5.

The resulting transmittance and phase modulation for both the scene and the filter SLMs are shown in Figure 2.29 and Figure 2.30 respectively. We present the theoretical prediction given by the modulation expression in equation 2.37, using the Márquez *et al* model for the TNLC, and also the experimental measurements for both the amplitude transmittance (Figure 2.29a for the scene and Figure 2.30a for the filter), and the phase modulation (Figure 2.29b and Figure 2.30b). The resulting operating curve in the complex plane is presented in Figure 2.29c and Figure 2.30c for the scene and for the filter respectively.

LCD	PSG			PSD		
	θ_P(deg)	θ_W(deg)	Γ(deg)	θ_P(deg)	θ_W(deg)	Γ(deg)
Scene	55	351	125	165	48	94.5
	71	45	125	297	324	94.5
Filter	60	11	50	179	76	88.0
	40	359	50	152	165	88.0

Table 2.5. Angles in degrees referred to the input director configuration for the spatial light modulators of the Scene and the Filter of the correlator.

One can observe a flat transmittance response, of about 0.8 in both modulators The phase modulation range of the phase is about 2π, this is an extremely good result if we take into account that the total birefringence of the panels is much lower: about

1.3π. Let us also remark the excellent agreement between experimental results and the theoretical predictions based on the obtained modulation function, and on the Márquez *et al* model of TNLCs.

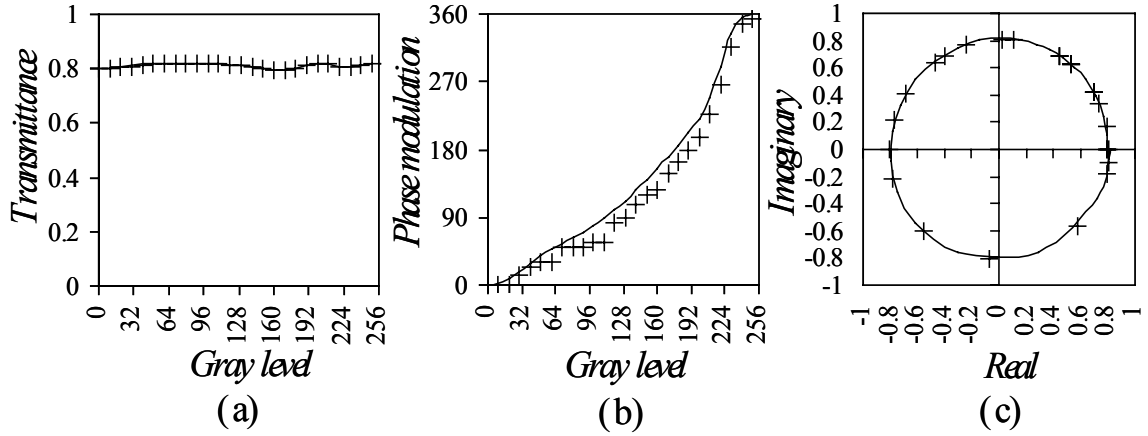

Figure 2.29. Response of the scene spatial light modulator in phase only mode. (a) Transmittance. (b) Phase modulation. (c) Operation curve.

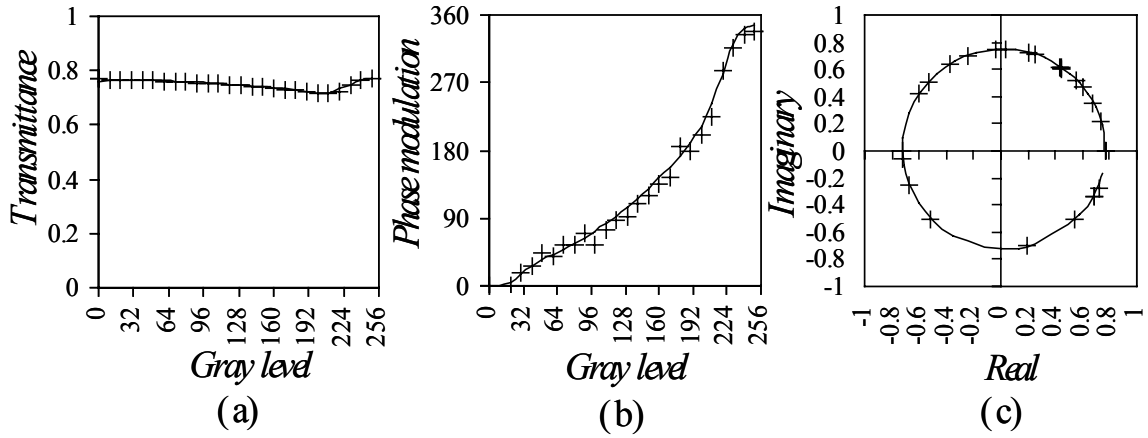

Figure 2.30. Response of the filter spatial light modulator in phase only mode. (a) Transmittance. (b) Phase modulation. (c) Operation curve.

2.8.Summary

We have demonstrated that it is possible to obtain amplitude only modulation or phase only modulation with a phase range

of 2π with a twisted nematic liquid crystal by using elliptical polarization.

The optimization method we propose presents several advantages: the dimensionality of the space of all the possible modulation responses is determined. So, the optimization uses the minimum number of parameters. In addition because there is no need to introduce any restriction to these parameters all the possible responses are included in the optimization method.

The expression of the amplitude and phase modulation is general for any SLM based on a linear device. This way, the technique can be extended for other kinds of polarization modulation systems, not only for image processing but also for diffractive optics or high speed optical fiber communications.

We determine the conditions that must be satisfied by the retarder plate of a PSG (or PSD) so as to reach the optimal polarization states and we give the procedure to obtain the configuration to generate or detect a given polarization state in terms of the parameters of the state and the retardance of the plate.